Final Report on NASA Contract NAS8-28055

Study of Design and Control of Remote Manipulators

Modeling Manipulator Arms with Distributed Flexibility for Design and Control

by

Wayne J. Book

Prepared by Department of Mechanical Engineering
Massachusetts Institute of Technology
Cambridge, Massachusetts, 02139

For George C. Marshall Space Flight Center, NASA
Marshall Space Flight Center, Alabama 35812

January 31, 1974

ABSTRACT

The interactions of control system and distributed flexible structural dynamics is explored for mechanical arms. A modeling process using 4 x 4 transfer matrices is described which permits the closed loop response of many current arm configurations to be evaluated. Root locus, frequency response, modal shapes, and time impulse response have all been obtained from the digital computer implementation of this model, which is oriented to arm design and allows for easy variation of the arm configuration through data cards. The model corresponds with experimentally observed natural frequencies with an average error of less than 5% in the first three flexible modes in the seven cases considered.

The model was used to explore the limits imposed by structural flexibility on a nondimensionalized two link arm with one and two joints for planar motion. Using simple position and velocity feedback and careful adjustment of control gains adequate damping (damping ratio of 0.65) can be imposed on dominant eigenvalues which have a complex modulus of more than one-half the cantilevered frequency of the arm with all joints clamped. The limitations imposed by flexibility are roughly compared to strength limitations to indicate when flexibility will tend to be the more immediate constraint on arm design.

Outline of Contract Report

Outline of Contract Report (con't.)

INTRODUCTION

The goal of this study was an improved understanding of the interaction of the various design components of manipulator arms so that arm design in the future would be based on more reliable and more logical procedures and tools. As a significant step towards that goal an arm modeling procedure has been established and implemented on the digital computer. This implementation is design oriented, allowing for easy alteration in the arm configuration and parameters. It focuses on an area previously ignored by design procedures: the flexibility of the various structural components and the interaction of that flexibility with the joint servo control to affect dynamic performance. The model implementation is based on frequency domain techniques and yields to the designer such information as natural frequencies, complex eigenvalues, mode shapes, the system frequency response in the form of Bode diagrams or polar plots, and via its inverse Fourier transform the time impulse response. This model has been verified with several experimental cases by comparing natural frequencies. It has been used to explore the interaction of structural and servodynamics for simple but reasonably general arm configurations. The rules developed appear to be reasonably valid for more complex models and thus as a first approximation for design.

Additional work has been done in expressing the laws of scaling for arms relating the mass moment of interia which limits gross motion speed to the limiting servo bandwidth which limits fine motion speed.

Arm Model

Since the arm model, its implementation and verification are an important product of this research, its rationale, features, verification and limitations will be discussed in some detail.

Modeling Rationale

Out of a number of possible models a selection has been made which results in features and limitations. The rationale for the selection will be discussed in the design context in which this study was carried out.

Small motions about a reference position. The most pervasive decision in the modeling process was perhaps to separate gross motions from small motions. This enables one to describe the arm as a linear system. The nonlinear

equations of motion for a rigid arm are quite complex and lengthy and the general flexible case seems beyond present capabilities. A linear model also allows for better comprehension of the issues of design. Aside from convenience one must discuss the validity and pertinence of a small motion model. The validity of the model to describe small motions is supported by the experiments discussed later. The pertinence of a small motion model to the design question is claimed on the basis of the following:

1) The frequency of structural vibrations is such that many cycles will occur before the configuration of the arm has significantly changed. Thus the interaction of the control system and structural flexibility is well described by a small motion model.

2) The first order effect of the gross motion on the structural arm vibrations can be represented by a disturbance loading, which is adequately described by the small motion model.

3) In most manipulator tasks the most stringent position accuracy requirements, therefore the most need for consideration of structure/servo interaction, occurs when the arm configuration is not rapidly changing.

Mixed Distributed Lumped Model. Observing manipulator arms of various designs one will find for general purpose arms one or more slender members which generally support the forces both transmitted to the payload and generated by the body forces of gravity and acceleration on the arm itself. Although these members are frequently not smooth enough to be called beams the contention here is that they can be modeled as such. Their compliance is most significant when supporting bending or torsional loads. If a significant portion of the mass of the arm is distributed throughout the length of this member, the distributed nature must be recognized in the modeling. The most straightforward approach is to describe the arm using partial differential equations. Alternatives such as lumping the mass and flexibility of the beam into separate elements approximate the distributed nature but require validation and tuning by checking with the corresponding natural frequencies of the distributed counterpart for example. This is especially cumbersome in design when the correspondence would be in doubt for each design parameter change.

A beam is considered to be distributed in one dimension only, which is reasonable for most arm models. It is conceivable that distributed effects in two or three dimensions would be important, but a model valid for design

purposes can be constructed in most cases without this complexity.

Other elements which are appended to the beam element such as joints, actuators, and some payloads seem to contribute essentially mass or essentially compliance and are more conveniently considered as lumped elements. The control action itself is concentrated at the joints of the arm and thus is well consided as lumped. The lumped parameter dynamics are described by ordinary differential equations and in this case the equations considered will be linear.

It is not intended to imply that by including distributed elements modeling the physical components of an arm or arm design will be without need for design judgement. Selecting from the possible model elements will improve with experience and the ultimate success of a model will depend on experimental fact.

Frequency Domain Model . Frequency domain techniques, while still a workhorse in many practical applications are not currently the vogue of controls engineers. State space models, with optimal control determined in the time domain are more popular and yield promise in many areas including manipulators. In the flexible arm design context they lack the versatility and ease of model construction and alteration that results with the present model.

The problem is especially acute with the mixed parameter problem at hand. Beam vibration control studies in the time domain have been published (1),(2), (3), for single uniform beams. A manipulator model based on a single distributed beam described in terms of its lower modes of vibration with control optimization in the time domain has been studied by Mirro[4]. When connecting two or more distributed beams the problem of boundary conditions between

---

(1) Koehne, Manfred, "Optimal Feedback Control of Flexible Mechanical Systems" Proceedings I.F.A.C. Symposium, Banf, Canada, 1971.

(2) Komkov, Vadim; "Optimal Control Theory for the Damping of Simple Elastic Systems", Lecture Notes in Mathematics No. 253, Springer-Verlag, 1972.

(3) Van de Vegte, J.. "Optimal and Constrained Optimal Controls for Vibrating Beams", JACC Atlanta, Georgia Session Paper 19-C, p.469. June, 1970.

(4) Mirro, John, "Automatic Feedback Control of a Vibrating Flexible Beam" SM thesis, MIT Department of Mechanical Engineering, August, 1972.

the systems of partial differential equations restricts time domain models severely. Lumped parameter models of flexible arms are discussed in (6).

Frequency domain techniques have long been available for beams but the technique is not frequently used in the context of control of distributed systems. The boundary condition problem is very conveniently solved utilizing the sequential (one dimensional) nature of beams and of arms in general. The numerical techniques are relatively straightforward. The lack of a mathematically convenient optimality criteria is not in itself a severe restriction since there is no concise definition of optimality for general purpose arms anyway. The frequency domain techniques will be discussed in more detail in a later section.

Arm Modeling and Implementation

This section will discuss the procedure used for modeling, its implementation, and the results that can be obtained.

Transfer Matrix Approach

The transfer matrix approach provides a versitile method of describing the interaction between the linear components of a system when that interaction occurs at no more than two stations of the component. For beams these two stations correspond physically to the two ends of the beam. For pure rotary springs these stations correspond to the ends of the springs. For rigid body inertias these stations correspond to the points of attachment. When three or more components interact at a single station it is still possible to use the transfer matrix approach if this interaction is well defined. The transfer matrix method is well explained by Pestel and Leckie[5] and only the essentials will be discussed here.

The interaction between two components is described by means of a vector of state variables. At the station between two components the value of the state variables is identical. A transfer matrix is used to describe the relation between the state variables at the two stations of each component. If the component is a static component (does not involve differentials with respect to time) such as an ideal spring, the transfer

(5) Pestel, Eduard C., and Leckie, Frederick A., Matrix Methods in Elastomechanics, McGraw-Hill, 1963

(6) Book, Wayne J., "Study of Design and Control of Remote Manipulators, Part II Vibration Considerations in Manipulator Design" NASA Contract NAS8-28055, N73-20138, Feb. 1973.

matrix is a function only of the component parameters. For dynamic components such as an ideal mass, the transfer matrix is also a function of the time derivatives of the state variables. For linear components (described by linear differential equations) it is convenient to deal with the Fourier transform of these equations which yields the steady state amplitude and phase (or complex amplitude) of the state variables under a pure sinusoidal excitation of frequency ω. The transfer functions for these components are functions of ω.

The state vector $\underline{z}$ that is used in the arm models consists of four variables displayed in Figure 1 for a beam with flexure in the x-z plane. These four state variables are sufficient to describe most arm vibrations of interest. Arm flexure in two planes can be described if these motions are decoupled. In addition torsional compliance of beams can be accounted for when vibrations out of the plane of two beams is studied. The sufficient conditions for decoupling the motion are discussed later. In general the neutral axis of the undeformed arm must lie in a plane for these four state variables to sufficiently describe the arm. Two link designs which predominate arms built today (except for short wrist segments) automatically qualify. Additional arm links or beam like supports modeled as part of the arm may of course be arranged in nonplanar configurations. There is no conceptual difficulty in extending the state vector to the complete three dimensional case. The twelve state variables then needed (flexure in two planes, twisting, and compression) lengthen numerical computation disproportionately to the information attained. State vectors with between 4 and 12 variables may give added information in some specific cases. Four state variables are all that will be considered here.

For decoupled motion it is sufficient for small motions that a planar arm have its joints either in or perpendicular to the plane of the arm, which is usually the case. For a typical arm two sets of data describe the small motions of the arm. One includes only flexure. The other includes distributed flexure and a lumped torsional compliance for out of plane motion. For arms that can be configured so as not to meet the requirements for decoupled motion an extended state vector or a configuration which does meet the requirements can be studied to obtain design information.

Given the transfer matrix B for a component and the state vector at one of its stations $\underline{z}_i$, the state vector $\underline{z}_{i-1}$ at the other station is given by the matrix multiplication.

$$\underline{z}_{i-1} = B\,\underline{z}_i$$

It is thus a simple matter when components are connected serially (two components per station except for the end components) to find an overall transfer matrix by multiplication of the individual matrices to eliminate the intermediate state vectors. This is demonstrated for an arm model in Figure 2.

The elements of the transfer matrices for various components are illustrated in Figure 3. The expressions are developed from the differential equation factored into time and space functions which can then be solved independently. The developments will not be given here but Figure 3 displays the results, many of which are developed in (5).

Model Implementation and Use

Included in this section will be a brief description of the computer programs used to implement the model including the basis for the computations, the type of input and output involved, and its meaning in the context of manipulator design.

Information available from the model includes natural frequencies, complex eigenvalues, the steady state frequency response, the inverse Fourier transform of this response which is the time impulse response, and the eigenfunctions which are the arm shapes when only one mode has been excited.

Numerical Operations with Transfer Matrices. The product of matrices such as appears in Figure 2 essentially is the implementation of the model of the arm which consists of beams, lumped masses, controlled joints and angles, joined end on end. The implementation of the model provides ways of getting useful information from that model. One possibility is to express analytically the elements of each component matrix, multiply the matrices and obtain a single matrix each element of which is a sum of products of the original matrix. While this is in fact done for a simple case in Appendix A, it is not recommended for more complex cases unless the same configuration is to be used many times. The alternative is to evaluate each term before the matrix product

is taken, then multiplying the numerical values. This is a procedure which can be carried out in a straightforward fashion by digital computer.

The advantage to numerical evaluation of this nature is that the complex functions need not be manipulated avoiding large amounts of designer time and potential for mistakes.

The disadvantages are of three types:

1) More computer time is required to evaluate expressions which might be simplified using trigonometric and hyperbolic identities. The simplification is not apt to be great unless there are identical components or at least many identical parameters. Additional computer savings may be observed when some of the transfer matrices have many zero or unity elements. Straightforward multiplication of these takes as long for the computer as do non-zero or non-unity elements. It may not be difficult for the designer to combine several simple elements into one matrix analytically if this combination is to be used frequently.

2) Numerical errors may become significant. The larger number of calculations may cause roundoff errors to become significant especially in some cases (evaluation of determinants) which require taking the difference of two large, nearly equal numbers. This difficulty has been encountered only in rare and unusual cases and been solved by using extended precision in those cases. It is also possible to get a numerical overflow in the product of the transfer matrices.

3) For simple cases the analytical expressions resulting from the matrix product may give the designer insight into the problem that the numerical results obscure.

Boundary Conditions and Forcing Functions. The transfer matrix, whether it describes a single component or a group of them, expresses the relation between the state variables at its two stations. In order for the transfer relation to be valid between state vectors, at most four of the eight state variables may be arbitrarily established. In fact for physical systems only two of the state variables at each station may be determined and more precisely for these state vectors only one of the associated variables of displacement or force and angle or moment may be arbitrarily specified. This specification may be as a simple boundary condition, as a forcing function, or as a linear combination of variables which may implicitly include the other

variables of the same state vector. This last case is in essence what one does when he appends another component by multiplying another transfer matrix. In this case one merely transfers the specification to another station in the extended system.

For simple boundary conditions one prescribes two non-associated variables of the arm. Figure 4 displays the physically possible combinations of zero state variables. The non-trivial solution of this case can result in solving for the natural frequency of complex eigenvalues (for damped systems). Additionally one can solve for the eigenfunctions of the system (the mode shape at the eigenvalue). The imposition of a forcing function yields the steady state forced response of the system, assuming the forcing function is a sinusoid of frequency ω. These techniques will be discussed in the following sections.

Natural Frequencies and Eigenvalues

If disturbed from the equilibrium position and then allowed to move freely after t=0 (without disturbance or outside input) the state variables of a linear system will be described over time by a function of the form

(1) $z_{i_k} = a_1 e^{j\omega_1 t} + a_2 e^{j\omega_2 t} + a_3 e^{j\omega_3 t} + \ldots a_i e^{j\omega_i t}$*

z_{i_k} = the i^{th} element of $\underline{z}_k$

For a lumped system there will be a finite number of these terms while a distributed system may theoretically have a countably infinite number.

For undamped systems the ω_i appear as the frequencies of vibration and assume real values. For damped systems some of the ω_i will have complex or pure imaginary values and it is more conventional to deal with the eigenvalues $s_i = j\omega_i$. Complex or pure imaginary values of s (complex or pure real values of ω) will always occur in pairs with the same real (imaginary) part and an imaginary (real) part with the same absolute value and opposite sign. When this is the case we will deal explicitly only with the value of s (ω) with the positive imaginary

* The assumption here is that the ω_i are distinct. For physical systems this is always true if one cares to look at the values with enough accuracy. The more general case $\omega_i = \omega_k$ does not restrict the results presented.

(real) part.

The values of ω_i for an arm system model depend only on the parameters of, and the boundary condition on, the system. They are independent of initial conditions, independent of which state variable is observed, and independent of the point in the system at which it is being observed. The values a_i depend on all of these quantities.

The time function (Eq. 1) which describes a state variable of the system must be consistent with the differential equations of the individual components, the general solution of which is the same form as Equation 1, also involving terms $e^{j\omega_i t}$. This general solution is the source of the transfer matrix for the component. For an isolated single component the rest of the rest of the system acts as a complex boundary condition which must be considered when determining the values of the ω for that component. The state variables between two components assume values over time that must conform with the general solution of two sets of differential equations. This can only occur if the values of ω are the same in both solutions and in fact the same as the general solution for the entire system.

The transfer matrix technique allows one to simultaneously consider all the components and the boundary conditions on the system and thus determine the ω_i of interest. Multiplying transfer matrices eliminates the intermediate state variables at the interface between components and expresses state variables at one end of an arm directly in terms of the other end. Imposing two boundary conditions at each ends restricts the values ω_i can assume for a nontrivial solution of the remaining state variables. These ω_i are the same ω_i appearing in Eq. 1. The restriction is developed in Fig. 5 for specific boundary condition on a specific arm model. In general for a system represented by a matrix product U such that

$$\underline{z}_0 = \begin{vmatrix} z_{10} \\ z_{20} \\ z_{30} \\ z_{40} \end{vmatrix} = U\underline{z}_n = \begin{bmatrix} u_{11} & u_{12} & u_{13} & u_{14} \\ u_{21} & u_{22} & u_{23} & u_{24} \\ u_{31} & u_{32} & u_{33} & u_{34} \\ u_{41} & u_{42} & u_{43} & u_{44} \end{bmatrix} \begin{bmatrix} z_{1n} \\ z_{2n} \\ z_{3n} \\ z_{4n} \end{bmatrix}$$

With the boundary conditions

$z_{i0} = z_{j0} = 0$ at station 0

and $z_{kn} \neq 0$, $z_{\ell n} \neq 0$ at station n

(implying the remaining two variables at station n are zero)

Requires for a nontrivial solution that the frequency determinant

$$2) \quad d = \left| \begin{matrix} u_{ik} & u_{i\ell} \\ u_{jk} & u_{j\ell} \end{matrix} \right|_{\omega = \omega_i} = u_{ik}\, u_{j\ell} - u_{jk}\, u_{i\ell} \Big|_{\omega=\omega_i} = 0$$

The elements of U and thus the terms of the frequency determinant are generally complex functions of ω . This being the case one must numerically search for values of ω where d=0. When dealing with systems with no damping one can restrict the search to real values of ω or complex values of the eigenvalue s. In general however, one must search over the complex plane for values of $s=s_i$, where both the real and imaginary parts of d are zero. In order to use conventional search routines one can search for minimum values of $\|d\| = \sqrt{(\mathrm{Im}\, d)^2 + (\mathrm{Re}\, d)^2}$, then check to see if d= 0+ j0 for the values of s returned. This topic will be discussed in more detail in a later section on numerical implementation.

Modal Shapes

Associated with each eigenvalue is an arm shape called the modal shape which describes the relative amplitide of all points of the arm when vibrating at that frequency. Looking at the problem from another perspective, there is an arm shape which when it constitutes the initial condition will result in arm vibration described by a single eigenvalue, to the exclusion of all other system eigenvalues.

The transfer matrix method can be employed to find the mode shape after the eigenvalue has been found. Refer again to the equation

$$\underline{z}_0 = U\,\underline{z}_n.$$

Two of the state variables at each end are specified by the boundary conditions, and the remaining four state variables can be solved for in terms of each other. By normalizing one of the state variables to be equal to one the remaining three are specified.

More specifically consider the boundary conditions resulting in Equation (2). The homogeneous equations which preceed the frequency determinant are

$$\begin{bmatrix} u_{ik} & u_{i\ell} \\ u_{jk} & u_{j\ell} \end{bmatrix} \begin{bmatrix} z_{in} \\ z_{jn} \end{bmatrix} = \underline{0}$$

If z_{in} is required to equal one, the solution for z_{jn} is

$$z_{jn} = \frac{-u_{ik}}{u_{i\ell}} = \frac{-u_{jk}}{u_{j\ell}}$$

Selecting the appropriate 2 x 2 submatrix from u will enable one to solve for the unspecified state variables at station 0.

In order to visualize the modal shape values of the state variables at intermediate points are helpful . For this one must refer to the transfer matrices of the separate components. For lumped components the knowledge of the state variable at either end is usually adequate for visualization. For distributed beams, however, the trigonometric and hyperbolic functions describing the shape within the component are far from obvious. For plotting

these functions one can essentially divide the component into smaller components thus creating additional intermediate state vectors (for purposes of plotting only, not for finding eigenvalues). When plotted versus distance along the axis of the arm the state variables indicate the shape, angle, moment and shear amplitudes along the arm.

Steady State Frequency Response

In the previous section two state variables at each end of the arm were specified to be equal to zero, thus establishing simple boundary conditions which enabled one to search for the eigenvalues of the arm system. Another way to specify the system is to impose sinusoidal forcing functions of frequency Ω and arbitrary but constant amplitude on from one to four of the state variables (subject to the same constraints on combinations of state variables as for boundary conditions indicated in Figure 4). The procedure here is actually more straightforward than for finding eignevalues.

Consider a linear system with at least a small amount of damping (present in all physical systems) forced by a single sinusoid of constant frequency for some appropriately long time. The response of that system at any point will be described completely by a complex amplitude times a sinusoid of the same frequency Ω. Alternatively the response could be described by a real amplitude and a phase angle. This complex amplitude as a function of Ω is termed the steady state frequency response.

Consider once again an arm model with describing transfer matrix u.

Now $$\begin{bmatrix} -w \\ \psi \\ M \\ V \end{bmatrix}_0 = U \begin{bmatrix} -w \\ \psi \\ M \\ V \end{bmatrix}_n$$

Assume the rows and columns of U are rearranged to form $\tilde{U}$ such that the first two state variables of the rearranged state vectors $\underline{z}_0$ and $\underline{z}_n$ are forced with a sinusoid of arbitrary but constant complex amplitude. Then

$$\underline{z}_0 = \tilde{U}\,\underline{z}_n$$

Let us partition this matrix expression such that

$$\underline{z}_0 = \begin{bmatrix} \underline{f}_0 \\ \underline{r}_0 \end{bmatrix} = \begin{bmatrix} \tilde{U}_{11} & \tilde{U}_{12} \\ \tilde{U}_{21} & \tilde{U}_{22} \end{bmatrix} \begin{bmatrix} \underline{f}_n \\ \underline{r}_n \end{bmatrix} = \tilde{U}\,\underline{z}_n$$

$\underline{f}_0$ and $\underline{f}_n$ contain the forced state variables and $\underline{r}_0$ and $\underline{r}_n$ contain the remaining state variables, termed the response variables.

3) $$\underline{f}_0 = \tilde{U}_{11}\ \underline{f}_n + \tilde{U}_{12}\ \underline{r}_n$$

4) $$\underline{r}_0 = \tilde{U}_{21}\ \underline{f}_n + \tilde{U}_{22}\ \underline{r}_n$$

solving explicitly for $\underline{r}_0$ and $\underline{r}_n$

from 3) $$r_n = \tilde{U}_{12}^{-1}\ f_0 - \tilde{U}_{12}^{-1}\ \tilde{U}_{11}\ \underline{f}_n$$

from 4) $$r_0 = \tilde{U}_{21}\ \underline{f}_n + \tilde{U}_{22}\ (\tilde{U}_{12}^{-1}\ \underline{f}_0 - \tilde{U}_{12}^{-1}\ \tilde{U}_{11}\ \underline{f}_n)$$

5) $$\begin{bmatrix} \underline{r}_0 \\ \underline{r}_n \end{bmatrix} = \left[\begin{array}{c|c} \tilde{U}_{22}\ \tilde{U}_{12}^{-1} & \tilde{U}_{21} - \tilde{U}_{22}\ \tilde{U}_{12}^{-1}\ \tilde{U}_{11} \\ \hline \tilde{U}_{12}^{-1} & -\tilde{U}_{12}^{-1}\ \tilde{U}_{11} \end{array}\right] \begin{bmatrix} \underline{f}_0 \\ \underline{f}_n \end{bmatrix}$$

Assuming U_{12}^{-1} exists.

Equation 5) expresses the four response state variables in terms of the four forced state variables. The value of ω at which the transfer matrices will be evaluated will be the forcing frequency Ω . The forcing vectors $\underline{f}_0$ and $\underline{f}_n$ will contain the (possibly complex and distinct) forcing amplitudes. Complex amplitudes can be used to represent a phase shift between the various forced state variables. $\underline{r}_0$ and $\underline{r}_n$ will contain the amplitudes of responses.

In practice it is seldom informative to force more than one state variable simultaneously. Then it is possible to simplify equation 5, assuming there is only one non zero element in $\underline{f}_0$ and $\underline{f}_n$.

Once again it is usually preferable to numerically evaluate the individual component transfer matrices prior to multiplication, enabling straightforward implementation on the digital computer.

Impulse Time Response

It is well known that the steady state frequency response is equivalent to the Fourier transform of the impulse time response for linear systems. This has long been used to obtain the power spectral density from time records. The inverse transform of the complex frequency response (which contains magnitude and phase information) can thus be used to obtain the impulse response. This enables one to visualize the system time response to an impulse disturbance. Thus if one desires the impulse response of a given state variable, displacement $w(t)$ for example, to an impulse disturbance at another state variable, sheer force V at the same station for example, one first uses Equation 5 to solve for the frequency response of that variable, in our example $w(j\omega)$. One then uses the inverse Fourier transform given by

6) $$z_{hi}(t) = \frac{1}{2\pi} \int_{-\omega}^{\infty} z_{hi}(j\omega)\, e^{j\omega t}\, d\omega$$

h = response state variable index

i = response station index

to determine the time impulse response for example w(t).

In practice we desire to evaluate this response digitally using discrete samples of both the time and frequency responses. This introduces a great number of subtle consequences which will not be discussed in this section. Suffice it to say that the inverse transform can be performed economically with a slight change in the very efficient FFT (Fast Foruier Transform) algorithm (7). The use of the algorithm in the inverse fashion is not well documented and will be discussed in a later section.

Experimental Verification of Arm Model

To get some indication of the accuracy of the model two sets of experiments have been performed. The first of these is summarized in Figure 6 and Table 1. The second is summarized in Figures 7 and 8 and Table 2. In both cases, the predicted natural frequencies of the undamped systems are compared to the resonant frequencies observed when forcing the system with a sinusiodal torque. In the first set of experiments, the frequency was determined via stroboscope. The second experiment was conducted by Octavio Maizza-Neto, also in the Department of Mechanical

(6) Bergland, G. D. "A Guided tour of the Fast Fourier Transform", IEEE Spectrum, July 1969.

Engineering at MIT. It was performed using automatic frequency sweeping and measurement of the amplitude of the endpoint of the system via accelerometer.

Table 1. Results of Experiment in Figure 6.

in or out of plane	Payload (slugs) (kg)	ℓ_1 (ft) (m)	ℓ_2 (ft) (m)	Φ degrees	predicted ω^1	measured ω^1	predicted ω^2	measured ω^2	predicted ω^3	measured ω^3
					ω (rad/sec)					
in	3.44×10^{-3} (.0502)	.921 (.281)	.885 (.270)	45	163	162	499	567	---	-----
out	3.44×10^{-3} (.0502)	.921 (.281)	.885 (.270)	45	157	161	549	565	1045	1025
in	1.12×10^{-3} (.0163)	.921 (.281)	.888 (.271)	45	233	232	556	605	1357	1350
in	0	.921 (.281)	.946 (.288)	45	263	264	585	635	1477	1464
in	3.44×10^{-3} (.0502)	.921 (.281)	.889 (.271)	0	201	211	520	583	1081	1100
in	1.12×10^{-3} (.0163)	.921 (.281)	.889 (.271)	0	260	268	596	643	1359	1377
in	0	.921 (.281)	.949 (.271)	0	284	292	631	667	1466	1481

average % error 4.1%

Table 2 Comparison of Predicted and observed (Fig. 7)

Natural Frequencies - Experimental Case

Model (hz)	Experimental (hz)	% Error
77.2	80.76	4.3%
145.0	136.6	6.0%
278	244.6	13.8%
477	{401.6 417.0}	{18.8% 14.4%}
795	688.3	15.6%
1063	{859.2 893.1}	{23.8% 19 %}
	1366	
	1591	

Figure 8 plots the acceleration amplitude measured versus frequency for this case.

The motor rotor inertia was the only value which could not be measured. Table 1 is based on values of that parameter taken from a motor catalogue. By using 30% lower values the maximum error was reduced to 3.7% for the first three natural frequencies. Thus it is possible that the errors in Table 1, although not excessive (averaging 4% do not do the model justice.

Predictions of the first three natural frequencies appear good in both cases, with accuracy decaying after that. Figure 8 displays acceleration amplitude.

The decay of the amplitude peaks indicate that the first two modes will dominate the response. This decay will be even greater for displacement amplitude. To obtain the relative magnitude of these peaks one must divide by the frequency squared. Table 3 shows the relative amplitude of the first six modes for acceleration and displacement.

Table 3 Relative Amplitude of First Six Resonances

Number	1	2	3	4	5	6
Relative Acceleration	1	.868	.162	.226	.166	.170
Relative Displacement	1	.304	.0177	.00914	.00229	.00150

The quality of the data seems good in both cases. The multiple peaks at some resonances in Figure 8 are probably due to the constantly changing frequency which does not allow the beam to reach steady state, and with the mixing of two nearly equal frequencies from the torque motor and the beams produces a beat like phenomenon.

For the higher modes a decay in accuracy is not surprising. Since the total motion involved in these vibrations is very small, nonlinear effects such as backlash from the nonzero tolerance at the joint become

Inverse Fourier Transform via Digital Methods

The calculations of the small motion response of the arm system have been carried out in the frequency domain. This information is related to the time domain response via an almost symmetrical pair of transformations -- the Fourier transform and its inverse. It is at best awkward to perform these transformations via analog hardware, and in view of the digital nature of the calculations to this point digital calculations are preferred. This introduces distortion due to sampling of continuous phenomena.

The digital Fourier transform (DFT) and its inverse have exact properties in themselves and can be used to approximate their continuous counterparts. This can be done most efficiently using the algorithm known as the fast Fourier transform or FFT to compute the DFT. Only by understanding the DFT can the sampled approximation yield information on the continuous case with the least distortion and greatest efficiency.

Fourier Series for Continuous Functions. For a periodic time function it is well known that there exists a representation in terms of a weighted sum of sines and cosines, or in terms of complex exponentials which are harmonics of the fundamental frequency Ω. This is called the Fourier series:

$$(7a) \qquad f(t) = \frac{1}{T} \sum_{i=-\infty}^{\infty} F_i \exp(j\Omega t) \quad i = \ldots -2,-1,0,1,2,\ldots$$

Where $j = \sqrt{-1}$

Ω = the fundamental frequency in rad/sec

more significant. Because of the small amplitude it is not felt that this significantly affects the model for practical use.

$$(7b) \quad F_i = \int_{-T/2}^{T/2} f(t) \exp(-j\, i\Omega t)\, dt$$

Where $T = 2\pi/\Omega$ = Period of one cycle in sec.

The F_i are the Fourier coefficients.

It is usually possible to truncate the series at a finite number of harmonics, which depends on the accuracy desired.

For aperiodic functions it seems intuitive that T goes to infinity and $\Omega = 2\pi/T$ goes to zero. In fact in the limit

$$(8a) \quad f(t) = \frac{1}{2\pi} \int_{-\infty}^{\infty} F(j\omega) \exp(j\omega t)\, d\omega$$

$$(8b) \quad f(j\omega) = \int_{-\infty}^{\infty} f(t) \exp(-j\omega t)\, dt$$

$F(j\omega)$ is the Fourier integral and is equivalent to the Fourier transform of the time signal.

The above are true for any time signals regardless of their origin. Certain additional relations will hold when the time function is the response of a linear system. When f(t) is the response of a linear system to an impulse input to one variable at a point in the system at t=0, $F(j\omega)$ is the steady state frequency response resulting from a unity amplitude sinusoid forcing the same variable. This is in fact what is obtained from the frequency domain arm model.

Discrete Approximations. Starting in either the frequency or time domain, one can at least formally transform to the other domain via Equations (8). In practice however one must approximate the transform by replacing the integration with summation and replacing the differential $d\omega$ with the increment $\Delta\omega$ resulting in

$$(9) \qquad f(t) \approx \hat{f}(t) = \frac{2}{\pi} \sum_{i=-n}^{n} F(ji\,\Delta\omega)\, \exp(ji\,\Delta\omega t)\, \Delta\omega$$

or

$$\hat{f}(t) = \frac{\Delta\omega}{2\pi} \sum_{i=-n}^{n} F(ji\,\Delta\omega)\, \exp(ji\,\Delta\omega t)$$

By comparing this with Equation (7) one realizes that this approximation must be periodic and of period $2\pi/\Delta\omega$, indicating that distortion of some sort has occured.

Certain steps must be taken to assure that the distortions resulting from the discrete approximations do not render the approximate time response $\hat{f}(t)$ useless. For $\hat{f}(t)$ to result from a stable physical system the response for $t<0$ (before any input) must be zero. Noting in Equation (8b) the two sided nature of the Fourier integral, and recalling the periodic nature of $\hat{f}(t)$ one can correctly conclude that the results of Equation (9) must be at least approximately zero for half of each period. This requires sufficient time for the impulse response to settle out, placing a lower constraint on the period $2\pi/\Delta\omega$ (or upper constraint on $\Delta\omega$).

It is not readily apparent in the frequency domain what an adequately small value of $\Delta\omega$ is. If one knows the location of the system eigenvalues he can estimate the settling time of each exponential. For complex conjugate root pairs for example

$$t_s \approx \frac{4\zeta}{\omega_n}$$

Where ζ = damping ratio of the root pair

ω_n = distance from origin of the pair

t_s = time to point where response remains within 2% of steady state

One may make $\Delta\omega$ smaller by either increasing the number of samples or by limiting the upper value of the frequency response considered. By lowering the upper value of frequency Ω_f that will be considered one removes the components of the time response with frequency greater than Ω_f. By looking at the frequency response for the system one can estimate Ω_f. Resonant peaks that are not down at least 20 db. from the magnitude at $\omega=0$ should be included if feasible. Thus for given settling times and given frequency Ω_f one arrives at a minimum sampling interval in the frequency domain analogous to the Nyquist sampling interval in the time domain. Just as small time intervals between samples are required to evaluate the frequency response for large frequency, small frequency intervals are required to evaluate the time response for long times.

Numerical Implementation

The arm modeling method has been implemented on a digital computer. This section will describe briefly the program and how the user may interact with it. Also described are numerical difficulties that have arisen in use and how they have been handled.

Computer Capabilities

Although it was originally intended to include all the programs in one package for interactive use by the designer, this goal has been abandoned for the present time due to the modest core storage of the machine used. The Interdata Model 70, with 40K 16 bit words of core storage at the M.I.T. Joint Civil-Mechanical Engineering Computer Facility was used. This is a mini computer handling interactive graphics and console input which is very useful in a design situation. An Interdata Model 80 with 32K 16 bit words of storage was used for some of the more extensive eigenvalue searches due to a lower price structure and a faster CPU. The program as it presently exists is divided into several compatible packages. Table 4 classifies the programs in seven more or less related categories. These could at some point be combined into an integral program with complete communication between all the program parts. Categories I, II, and III utilize descriptions of the arm and subroutines in VI and VII Categories IV and V use output from II and III to obtain additional information.

Nature of User Input

This section will briefly describe the nature of the user input to the system to indicate the designer effort required (not to indicate how to use the programs).

Table 4. Program Category Outline for Numerical Implementation

I Natural frequency calculation (no damping)

- A. Single Precision
- B. Double Precision

II Eigenvalue search (two dimensional search, systems with damping)

- A. Card and console input only
- B. Interactive graphics implementation

III Frequency response calculation

- A. Logarithmic frequency scale
  - 1. Bode plot
  - 2. Polar (Nyquist) plot
  - 3. Modified polar plot
- B. Linear frequency scale (equal increment in frequency for FFT input)

IV Mode shape calculation and display

V Fast Fourier transform

VI Component transfer matrix calculation

- A. Distributed Beam
  - 1. Bernoulli -Euler model
  - 2. Timoshenko model (includes shear and rotary inertia)
- B. Rigid Body
  - 1. General
  - 2. Uniform cross section
- C. Angle in the arm shape
  - 1. In the plane of vibration
  - 2. Perpendicular to the plane of vibration
- D. Controlled Rotary Joint
  - 1. Transfer function control

2. With flexible shaft and gear reduction.

E. Parallel elements (combines certain elements in parallel by clamping them at each end).

F. Discontinuity in one state variable (with its associated variable equal to zero eg. pinned connection between beams or pinned connection to ground)

VII Search Routines

A. Pattern search - 2 dimensional

B. IBM SSP root finding algorithm

Arm Description. The description of the arm to be modeled is in terms of the arm elements or components selected from Category VI of Table 4. Each element requires one and sometimes more data cards giving its parameters and are arranged in the order of occurance on the arm. In certain cases there are restrictions as to what combinations of elements can be used. For instance angles in and out of the plane of vibration would result in a nonplanar arm which cannot be handled by four state variables. Other restrictions include 1) arm discontinuity can be used only with natural frequency or eigenvalue (I and II) calculations as presently implemented.

2) Parallel elements cannot be used with mode shape calculations.

3) Flexible shafts incorporated into the controlled joint must connect to a pinned, clamped, or sliding end of the arm.

Calculation Description Input. Presently the description of the desired calculation for natural frequencies and frequency response requires one card for describing arm boundary conditions, calculation type, number of increments, and extreme frequencies considered. In addition the forcing variable must be specified for frequency response calculations. A number of selections of output alternatives and extended calculations are available by data switch and console input at run time.

For eigenvalue calculations additional starting points for the two dimensional search can be read in from card or console in one implementation, or input graphically via joystick and crosshairs in another implementation.

Mode shape calculations require the input of the eigenvalues for the system for the mode for which the shapes are to be calculated, boundary conditions, and the number of points at which the shape is to be calculated for each beam element.

To calculate the inverse Fourier transform to obtain the time impulse response, the frequency response must first be calculated with equal spacing between calculations (IIIB). The results are stored on disc to be used by the FFT algorithm. The specification of the total number of points to be used and the frequency range they cover is input by card.

Nature of Program Output

The program output is of the nature described in Table 4. In cases where there are arrays of data (such as the values of frequency response) this data can either be plotted or plotted and printed to allow more precise comparisons. In this case there is also a selection of which endpoint state variables are to be plotted. The three types of frequency plots are the Bode diagram, Polar plot of magnitude vs. phase, and the modified polar plot which can be used in stability analysis for certain nonlinear arm elements. The graphics assisted eigenvalue search program also yields a plot of the roots as they are found.

Numerical Difficulties

The arms modeled to date have resulted in few numerical difficulties. The difficulties encountered and ways of dealing with them are described below.

False Roots in Eigenvalue Search. For a damped arm system the frequency

determinant is a complex number. Evaluated at the system eigenvalue both real and imaginary parts should be zero. Since conventional root finding algorithms deal only with real values, alternative methods must be found. At present the procedure is to minimize the complex modulus via a pattern search program developed by Prof. D.E. Whitney. The global minimums must be zero, but the search routine may return false eigenvalues corresponding to local minimums. These can usually be detected by simply looking at the modulus value. When the modulus value is near zero there is a possibility that the nonzero determinant is due either to the finite word size of the computer or to the fact that a false root has been returned. To resolve this ambiguity one can look at the real and imaginary parts of the determinant. If an actual system root has been returned, and it is a single distinct root, the real and imaginary parts must both change signs in the neighborhood of the root. In normal operation where the change in roots with design changes is being observed the user confidence in root positions is high, and only when unexpected root locations are returned is the doubt sufficient to check the sign change. The experience has been that this check seldom fails to confirm a root whose determinant value was reasonably low (say less than 0.1). What is considered "reasonably low" varies with the arm and the position of the root.

Convergence to the "Wrong" Eigenvalue Since the eigenvalue search bases its actions on the shape of the determinant modulus over the complex plane, it will converge to different roots depending on where the search is begun. Thus one can repeatedly "find" the same root and not find a desired root. Under these circumstances graphical display and input becomes very helpful, allowing the user to quickly modify the starting point of the search based on the displayed results

of the previous search. Search routines specifically designed to take advantage of the particular problem of complex root finding might do much better and cut down on the user interaction required.

A more critical numerical problem arises when it is practically impossible to make the routine coverage to a root that exists. This has been observed for extreme values of arm servo control parameters. It corresponds to shapes of the determinant that change very rapidly in the region of the eigenvalues. It seems to be aggravated by two roots which are very close. Fortunately when this happens it also seems that the root changes very slowly with parameter changes so that roots determined with different parameter values can be used.

Numerical Overflow In only one case has the problem of numerical overflow been encountered. The problem was solved for that case by using extended computer word size, which may not be practical in all cases for all computers.

PART II

Characterization of the Arm Servo -- Structure Interaction
Two Equal Link Example

In an effort to characterize the interaction of the joint servo control and the structural flexibility of typical arm configurations the following study was undertaken. The most typical of general purpose arm configurations seems to be one with two long beam like segments of approximately equal length with rotary joints. An additional short segment incorporating the end effector is also typical but will not be considered in this study.

The beam segments in this study are considered to be identical in all properties but have different boundary conditions. They are joined by a servo controlled rotary joint. This "elbow" joint is assumed to operate on the position and velocity error feedback of the joint, analagous to a rotary spring and dashpot. One end of the two link arm has free boundary conditions and the other end is clamped to ground in the first case, and in the second case is connected to ground via a rotary "shoulder" joint with the same control scheme as the elbow joint.

The modeling process discussed in Part I was used to obtain the dynamic characteristics of the two cases. The display of the dominant eigenvalues is relied on heavily to convey the changes in system behavior due to changes in joint servo control parameters. In some cases this is supplemented with the frequency response and time impulse response due to end point force distrubances. The frequency determinant was analytically simplified for this study as described in Appendix A.

Two Link, One Joint Case

First let us consider the two identical link, one joint case illustrated in Figure 9. This case includes distributed beam dynamics on either side of a controlled joint. It proves to be very informative because after nondimensionalization the results for the complete range of independent parameters can be displayed on one plot of the root loci.

Nondimensionalization of Parameters

Table 5 displays the important physical parameters for this problem and a set of convenient nondimensional groupings. They are nondimensional frequency (complex) $\bar{\omega}$ which is multiplied by $\sqrt{-1}$ to obtain the eigenvalue, the nondimensional servo frequency $\bar{\omega}_s$ and damping ratio ζ. The servo frequency would result from a rigid inertia equivalent to that of the outer link with only the joint position feedback.

As observed in Figure 10 and in Figure 11 in more detail this simple case has root loci which fall into three characteristic groups as follows:

1. $\bar{\omega} \ll .386$
2. $\bar{\omega} \approx .386$
3. $\bar{\omega} \gg .386$

Appearing in Figure 12 are the higher order roots that are not dominant.

Low Servo Bandwidth (Figures 10a and 11a)

For case 1 with $\bar{\omega}_s$ much less than .386 rad./sec. and ζ not much greater than 1.0 the behavior is essentially that of a rigid arm. For $\zeta < 1$ the complex conjugate roots r_1 and r_2 near the origin indicate oscillatory behavior. For ζ just greater than one the real roots indicate overdamped behavior. There will theoretically also be vibrations of an infinite number of modes of the distributed beams. Their effect will be less important in most cases because their time constants are several times higher and their amplitudes several times lower than the lower, dominant modes. As ζ is increased past one, one of these real roots, r_1, moves toward the origin and r_2 moves away from the origin, eventually meeting a third root, r_3, moving toward the origin. Further increases in ζ cause r_2 and r_3 to become complex. As ζ gets very large these roots move in an arc and approach the imaginary axis. The value they approach is the clamped elbow natural frequency of the arm, which is the value one on the vertical axis of the nondimensional plot of Figure 11.

Table 5. Nondimensional and Physical Variables for the Two Flexible Link, One Joint Case

Physical Variables	Nomenclature	Dimensions
Joint position feedback gain (angular)	k	LF
Joint velocity feedback gain (anular)	c	LFT
Frequency (complex)	ω (-js)	T^{-1}
Mass density / unit length	μ	FT^2L^{-2}
Total arm length	ℓ	L
Stiffness product	EI	FL^2

(E = Young's modulus and I = cross sectional area moment of inertia)

From these variables we construct for convenience:

First natural frequency of a cantilevered beam of length ℓ

$$\omega_c = 3.52\sqrt{\frac{EI}{\mu\ell^4}}$$

Servo frequency for a rigid arm structure

$$\omega_s = \sqrt{\frac{24\ k}{\mu\ell^3}}$$

If one replaces EI and μ as independent dimensional parameters with ω_c and ω_s, one can form the following nondimensional groups:

Nondimesnional Variable	Nomenclature	Grouping
Frequency	$\bar{\omega}$	ω/ω_c
Servo frequency	$\bar{\omega}_s$	ω_s/ω_c
Servo damping ratio	ζ	$\frac{12\ c}{\mu\ \ell^3\ \omega_b}$

Critical Servo Bandwidth (Figures 10b and 11b)

As $\bar{\omega}_s$ is increased, the point at which r_1 and r_2 join the real axis, and the point at which r_2 and r_3 leave the imaginary axis move closer together. For a critical value of $\bar{\omega}_s$ found numerically to be about 0.386 these two points meet and there exists a triple root for $\zeta \approx 0.915$ in the region of $(-.67 + j0.0)$. In this region the position of the roots is very sensitive to slight variations in $\bar{\omega}_s$ and ζ. This critical point seems to be the farthest from the origin that the nearest root of the arm can be located, and thus the fastest overdamped response of these dominant roots obtainable with simple joint position and velocity feedback.

High Servo Bandwidth (Figures 10c and 11c)

For $\bar{\omega}_s \gg 0.386$ the root locus plot looks quite different than for $\bar{\omega}_s \ll 0.386$. A single root r_3 remains on the real axis moving toward the origin as ζ increases. The two complex conjugate roots r_1 and r_2 remain imaginary for all values of ζ. They move from a value on the imaginary axis for $\zeta=0$, through an almost semicircular path to a point whose value is the clamped elbow natural frequency. As $\bar{\omega}_s$ becomes larger the semicircles become smaller and the real root becomes more negative for the same value of damping ratio ζ. In this region the spring is too stiff to allow motion which would dissipate the vibrational energy of the beam. This is essentially a poor match between the mechanical impedances of the structure and joint for the purposes of dissipating energy.

Conclusions and Summary for Two Link, One Joint Case

Figure 11d displays contours of constant position feedback gain

(equivalent to constant $\bar{\omega}_s$) for a wide range of values of $\bar{\omega}_s$. Also indicated in dashed lines are the contours of constant ζ. This plot shows the transition from the rigid to the floppy extreme cases for the lowest complex conjugate pair.

Conclusions one might support with a graph of this type include:

1) Through careful design one may be able to achieve dominant system eigenvalues on the order of one-half or more of the lowest clamped joint natural frequency using this simple control. For example see $\omega_s/\omega_c = 5$, $\zeta = 0.8$.

2) Noticeable deviations from rigid behavior become apparent when the eigenvalues of the rigid dynamics are of a magnitude of about one-fourth the lowest clamped joint natural frequency. For example see $\omega_s/\omega_c = 0.33$. Excitation of the higher modes by periodic excitations may require that flexibility be considered for any arm.

3) Consideration of arm flexibility becomes crucial when a rigid design procedure produces dominant eigenvalues the magnitude of which is greater than one-third the lowest clamped joint natural frequency. A rigid analysis of the behavior would indicate that increased velocity feedback would result in increased damping on the dominant complex root pair. The opposite result occurs in the actual flexible system and the effect is to decrease damping for the complex conjugate pole pair. See for example $\omega_s/\omega_c = 0.5$, $\zeta = 0.8$.

The case for two joints with this same control scheme discussed in the following section supports these conclusions. Additional factors which should be considered are unequal beam cross section, payload and actuator masses, and a more sophisticated control.

Two Link, Two Joint Case

Having considered the two link one joint case the next logical step in complexity is two links and two joints. This configuration more resembles an actual manipulator although when the additional joint is locked or if the joint drive is self locking and not being driven the previous result is more realistic. The step is made with considerable increase in the difficulty with which one can thoroughly understand the case. With the simplifying assumptions of identical links and feedback constrained to two variables per joint one must deal with four independent parameters in the flexible case after nondimensionalizing the problem and establishing the nominal joint angles about which vibration is being studied. While this is not so great as to prohibit meaningful exploration of the case, it makes compact and intuitive display impossible.

Limiting Case - Rigid Links

In order to establish bounds for the flexible link behavior we will first consider the limiting case of rigid links. In one nominal position this case can be described by three nondimensional parameters as shown in Table 6. As chosen here these correspond to nondimension gains in the feedback of the velocity and position of the proximal or shoulder joint and the velocity of the distal or elbow joint. The problem is nondimensionalized with respect to the total arm length, the elbow position feedback gain and the undamped natural frequency with the shoulder joint clamped.

Lagrange's equations were used to develop the frequency function for the rigid link case and that development is sketched briefly in Appendix B. For the constrained feedback the rigid motion is very

close to that of a double pendulum for small vibrations.

Nondimensionalization of Two link, Two Joint Example

By nondimensionalizing the two equal link, two joint case we can reduce a problem of eight parameters to one of five parameters. For root locus plots one of these parameters is the location of the roots which will be a function of the other four parameters. The choice of nondimensional groupings will depend on convenience and the physical significance to the problem at hand. In the case of two links and one joint the choice was influenced by the prior understanding of a simple second order system which was the limiting case as the links became very rigid relative to the joint. When two joints are present the rigid counterpart is a fourth order system which is generally not nearly so intuitively comforting.

By retaining nondimensionalization compatible with the rigid analysis, however, we can draw on our previous analysis and readily see when there is a significant departure from the rigid behavior. Thus we chose the nondimensional groupings of Table 7 which enables us to see in what range of flexibility the rigid analysis is valid. Notice we can move from the rigid analysis whose parameters appear in Table 6 to the flexible analysis by additionally specifying one value, the ratio of the clamped joint, cantilevered frequency to the rigid (clamped shoulder) frequency, $\omega_c / p = \bar{\omega}_c$.

Table 8 shows alternative parameters that will be used for improving on the rigid analysis when the links are significantly flexible.

Table 6 Nondimensional and Physical Variables of the Two Rigid Link, Two Joint problem

Physical variables	Nomenclature	Dimensions
Distal Joint position feedback gain (angular)	k_2	FL
Distal Joint velocity feedback gain (angular)	c_2	FLT
Proxal Joint Position feedback gain (angular)	k_1	FL
Proxal Joint velocity feedback gain (angular)	ℓc_1	FLT
Mass Density / unit length	μ	$FT^2 L^{-2}$
Total Arm length	ℓ	L
Frequency	ω	T^{-1}

Construct the following variable equivalent to the natural frequency of the arm with the proximal joint clamped, and with simple position feedback of gain k_2 to the distal joint with dimensions T^{-1}.

$$P = \sqrt{\frac{24k_2}{\mu \ell^3}}$$

Nondimensional variables	Grouping of Physical variables
$\bar{\omega}$	ω/p
$\bar{k}$	k_1/k_2
$\bar{c_1}$	$c_1 \ell c/k_2$
$\bar{c_2}$	$c_2 \ell c/k_2$

Table 7. Nondimensional and Physical Variables of the Two Flexible Link, Two Joint Case. (For deviation from rigid analysis.)

Physical Variables	Nomenclature	Dimension
Distal joint position feedback gain (angular)	k_2	LF
Distal joint velocity feedback gain (angular)	c_2	LFT
Proximal joint position feedback gain (angular)	k_1	LF
Proximal joint velocity feedback gain (angular)	c_1	LFT
Frequency (complex roots)	ω	T^{-1}
Mass density/unit length	μ	FT^2L^{-2}
Stiffness product (E = Young's modulus, I = cross section moment of inertia)	EI	FL^2
Total arm length	ℓ	L

From these physical variables we construct for convenience:

First natural frequency of a cantilevered beam: $\omega_c = 3.52\ \sqrt{(EI/\mu\ell^4)} \triangleq T^{-1}$

Rigid natural frequency with proximal joint clamped: $p = \sqrt{3k_2/\mu\ell^3} \triangleq T^{-1}$

We will use the variables ω_c and p instead of EI and μ and nondimensionalize with respect to p, k_2, and ℓ to obtain the following groupings :

$\bar{\omega}$	ω/p
$\bar{k}_1$	k_1/k_2
$\bar{c}_1$	c_1p/k_2
$\bar{c}_2$	c_2p/k_2
$\bar{\omega}_c$	ω_c/p

Table 8. Nondimensional and Physical Variables of Two Flexible Link, Two Joint Case. (Constant link parameters.)

Physical Variables	Nomenclature	Dimension
Distal joint position feedback gain (angular)	k_2	LF
Distal joint velocity feedback gain (angular)	c_2	LFT
Proximal joint position feedback gain (angular)	k_1	LF
Proximal joint velocity feedback gain (angular)	c_1	LFT
Frequency (complex roots)	ω	T^{-1}
Mass density/unit length	μ	FT^2L^{-2}
Stiffness product (E = Young's modulus, I = cross section moment of inertia)	EI	FL^2
Total arm length	ℓ	L

From these physical variables we construct for convenience:

First natural frequency of a cantilevered beam: $\omega_c = 3.52\sqrt{(EI/\ell^4)} \stackrel{d}{=} T^{-1}$

Cantilever beam endpoint rotational spring constant: $\alpha = EI/\ell \stackrel{d}{=} LF$

Use ω_c and α instead of μ and EI. Nondimensionalize with respect to ℓ, ω_c, and α to obtain:

$\bar{\omega}$	ω/ω_c
$\bar{k}_1$	k_1/α
$\bar{k}_2$	k_2/α
$\bar{c}_1$	$c_1\omega_c/\alpha$
$\bar{c}_2$	$c_2\omega_c/\alpha$

Performance Criteria

When dealing with the flexible or rigid case one needs to develop some criteria for good dynamic performance. While some criteria are obvious such as stability, others depend on the specific application of the arm and in the practical design case are almost always the result of a combination of subjective designer opinion and constraints of weight, power, or previous design decisions. The quadratic cost function of linear optimal control is a popular way to specify performance but is more the result of mathematical convenience than a correct estimation of the cost.
For an indication of how different criteria can result in different systems refer to Figure 13. It displays eigenvalues of optimal fourth order systems by three criteria: Integral of Time times Absolute Error (ITAE), Solution Time criterion, and a quadratic cost function developed by Townsend[7] for manipulator arms. Townsend's control gains resulted in all overdamped roots and a rather sluggish system, The other two criteria , ITAE and solution time, result in four underdamped roots and therefore a much faster response, but with some overshoot.

In an effort to make this analysis independent of the criterion selected the roots of the arm in a broad range of configurations which might be termed acceptable will be discussed.

The transient performance of systems with various root pole placements and desirable placements for poles is extensively discussed by Graham and Lathrop.[8]

---

(7) Townsend, Allen L. Jr., "Linear Control Theory Applied to A Mechanical Manipulator" SM thesis, Dept. of Mechanical Engineering, Massachusetts Institute of Technology, January, 1972

(8) Graham, Dunstan, and Lathrop, R.C., "The Synthesis of 'Optimum' Transient Response: Criteria and Standard Forms". Transactions of the AIEE Vol.72 part 2, November, 1953.

Feedback Control Configuration and Its Limitations

As suggested previously the control configuration which is being considered in this section is not complete state variable feedback, even in the rigid case. This would involve feedback between the joints (interjoint feedback) as well as within the joint (intrajoint feedback). Four additional feedback gains would be involved, two velocity and two position gains. The additional complexity would enable complete freedom in the rigid case of placing the eigenvalues of the system where ever desired and in some arms the improved performance may well be worth the added complexity. Such interjoint feedback is extremely rare in arms produced today, even experimental arms. In fact many arms do not have velocity feedback and are dependent of friction in drive trains which is highly variable from unit to unit, and cannot be readily controlled.

Thus while we can achieve many acceptable pole placements it would be accidental if we could achieve the optimal, even if that optimum were validly and precisely defined. For example we cannot match the eigenvalues dictated by the standard forms of the ITAE or solution time criteria or in general duplicate the eigenvalues of a quadratic cost optimal system. More complete feedback would give one more degrees of freedom in placing system eigenvalues arbitrarily, freedom not available in the present case. The feedback gains determined from the matrix Riccatti equation for a quadratic cost criterion for example assumes all measured state variables can be fed back to any control variable.

The justification for this simplificaiton then is that it more adequately describes the practical problem. This constraint in feedback is not entirely a simplification. Design techniques for complete state variable feedback are more readily available than for restricted feedback.

Discussion of the Root Loci-Two Link, Two Joint Rigid Link

Figure 14 displays the location of the complex conjugate root pair for the case in question with no veolcity feedback or damping. We will reference the roots as r_1, r_2, r_3, and r_4 where $r_1 = r_2^*$ and $r_3 = r_4^*$. The lower indexes refer to roots nearer the origin. The relative position of the damped roots is determined by the ratio of postion feedback at the two joints k_1/k_2 . This relation is displayed in Figure 15. In the nondimensional case considered the lower root asymptotically approaches 1 as the inboard "spring" k_1, is made stiffer, k_2 remaining fixed at 1. The position of these roots is moved to the left as the velocity is fed back with increasing negative gain. The series of Figures 16a through 15d shows these variations in detail.

For any value of k_1/k_2, the roots can be brought to the negative real axis by increasing c_1 and c_2 appropriately. The difficulty arises in achieving sufficient damping for the pair r_1 and r_2 without greatly overdamping roots r_3 and r_4. For relatively low values of k_1/k_2 (see Figure 16a) it is impossible to achieve a damping of the order of 0.7 on r_1 and r_2 without bringing the roots r_3 and r_4 down to become two real roots, one of approximately the same magnitude as r_1 and r_2. For values of $k_1/k_2 = 2$ a reasonable response can be obtained of a third order nature for $c_1 = 6.5$ $c_2 = 0.1$. As noticed in Figure 16, r_1 and r_2 are much nearer the origin but this can be compensated for by increasing k_2 when dimensional values are completed, thus shrinking the scale of the plot.

As k_1/k_2 is increased to 5 and 10, higher values of c_2 are required to damp the lower modes sufficiently. The high values of both c_1 and c_2 in turn overdamps the higher modes. bringing a slow real root near the origin. However, as k_1/k_2 continues to increase to 50 (see Figure 16d) the lower mode becomes essentially independent of c_1, and its damping can be controlled by c_2 at will. This approaches the one joint case. For $k_1/k_2 = 50$, $c_1 = 2$, $c_2 = 1.7$ the two complex conjugate pairs will both have damping greater than 0.7.

Thus there are many parameter values where performance might be satisfactory. The one perferred would depend on the application at hand. The area with k_1/k_2 large seems preferrable in terms of performance but the higher gains would require larger shoulder motors if the operation is to remain within

the linear range. This is feasible however. It may be difficult to achieve the low values of damping desired at the joints especially when large gear reductions are involved.

When k_1/k_2 is small (the two gains are more nearly equal), the lower pair of roots remains much nearer the origin. (Figure 16a). To have a response of comparable speed in a system with this control it is necessary to have a higher k_2, which has the effect of shrinking the nondimensional scales of Figure 16. This may not be desireable since a larger value of k_1 requires more torque if the response is to remain linear. This requires more massive motors and drives at the outer joint, or compliant transmission shafts which aggravate the vibration problems.

Shift from Rigid Roots for Flexible Links

To demonstrate the change of the roots as the links become more and more flexible, examples were chosen from the rigid case which had reasonable root locations. Appearing in Figure 17 are the following cases, nondimensionalized as in Table 7.

$\bar{k}_1 = 2$	$\bar{c}_1 = 5$	$\bar{c}_2 = .5$
$\bar{k}_1 = 10$	$\bar{c}_1 = 15$	$\bar{c}_2 = 2$
$\bar{k}_1 = 50$	$\bar{c}_1 = 10$	$\bar{c}_2 = 1.7$

For each case the stiffness parameter of the arm ω_c is varied from one to 10 and the root position is plotted. This is not presented as evidence of the limits of flexibility for reasonable performance, but as evidence of the limits of a rigid design procedure. As ω_c decreases the complex conjugate root pair, r_1 and r_2 become less damped in all cases, moving from the position of the rigid root. The real root near the origin in these cases moves nearer the origin indicating a slower response. For $k_1 = 10$ it is observed that the rigid root near the origin does not move but an additional real root moves in causing similar effects of slower response and increased phase shift.

Several things can be observed qualitatively from these three examples. Higher values of position feedback k_1 result in the complex conjugate pair being more sensitive to ω_c. Initially one might think that this favors lower k_1 for more flexible links. This is not conclusive since to get a comparable

speed from the two systems $\frac{k_1}{k_2}$ = 10 and k_1/k_2 = 50 one would have to use a larger value of $p = \sqrt{3\, k_2/\mu \ell^3}$ when moving to dimensional parameters. If one used p = 2 for the case k_1/k_2 =10, ω_c =ω_c p would also double. The present nondimensionalization scheme indicates limits of the rigid analysis but is not well adapted to improving on that analysis. For this reason a slightly different scheme will now be used which fixes the links while allowing us to vary all the parameters of the joint control system.

Improvement on Control with Constant Flexible Link Parameters In order to demonstrate how one might improve on the servo control parameters using the flexible model we will take an example from Figure 17. First we will convert from the nondimensional parameters of Table 7, which allowed ease in comparison to the rigid case, to the nondimensional parameters of Table 8, which holds the structural parameters constant and displays directly what we can accomplish with the control. The case chosen for demonstration is:

Variable Structural Parameters	Constant Structural Parameters
(Table 7 and Figure 17)	(Table 8 and Figure 18)
$\bar{k}_1$ = 50	$\bar{k}_1$ = 6.5
$\bar{\omega}_c$ = 2	$\bar{k}_2$ = 0.13

First the velocity feedback gain $\bar{c}_2$ to the outer joint is varied until a maximum damping on the complex root pair is found as shown in Figure 18. Then $\bar{c}_1$, the velocity feedback to the inner joint is varied until the slow real root moves in, slowing the response. If the maximum damping ratio shown in the figure of 0.58 is not adequate for the application at hand, other values of k_1 and k_2 could be tried or the slow real root with slow response would have to be tolerated.

Effect of Structure Dynamic Rigidity Requirements on Gross Motion Speed

The locked actuator natural frequency of an arm can be increased by a redistribution of mass as well as by making the entire arm more rigid. This may involve a tapered structure of relocation or actuator masses. This relocation requires power transmission channels such as shafts, cables, or hydraulic lines which add both weight and compliance, at least partially offsetting the improvements.

When it is necessary to increase the structure's cross section size in order to increase ω_c, gross motion times suffer as described below. The value of ω_c increases linearly with r, the radius of the structure's cross section, and the inertia of the arm increases as r^2. The task time t_f to perform a gross motion of given angle can be shown to increase as r and thus as ω_c assuming no gravity and a bang-bang control strategy with maximum torque T_m.

One might consider what penalty one must pay for operating conservatively at a smaller ratio of ω_s / ω_c than is necessary. Consider moving from the limiting case of $\omega_s / \omega_c = 0.5$. to the slightly conservative case of $\omega_s / \omega_c = 0.3$, by increasing r, with a damping ratio of .65 in both cases. In the limiting case the nondimensional root is 80% farther from the origin than the conservative case. This operating at $\omega_s / \omega_c = .3$ would require an 80% larger value of r at the expense of an 80% increase in gross motion time.

The minimum value of r established by strength considerations may be larger than the minimum required to yield a sufficiently high value of ω_c. For a bending moment T_m applied to a beam, we can show that the minimum value of cross sectional radius r_{min} is proportional to $T_m^{1/3}$ and that

$$(10) \qquad \omega_{c,min} \quad \alpha \quad \frac{r_{min}}{\ell^2} \quad \alpha \quad \frac{T_m^{\frac{1}{3}}}{\ell^2} \quad .$$

where ℓ is the total length of the arm.
As discussed previously ω_c determines the minimum settling time and thus the fine motion control speed. A comparable gauge of gross motion speed with bang-bang control of the second link inertia is

(11)

$$\frac{0}{t^2_f}_{min} \propto \frac{T_m}{\ell^3 \, r^2_{min}} \propto \frac{T_m^{\frac{4}{3}}}{\ell^{1.3}} \quad .$$

It is postulated that there exists a preferred ratio of gross motion speed to fine motion speed. If so, equations (10) and (11) might indicate when the structure cross section is lower bounded by the gross motion speed requirements (via maximum torque) and when it is lower bounded by the fine motion speed requirements (via ω_c). Viewed alternatively it might indicate

when we must increase r from r_{min} to achieve an adequate value of ω_c. As T_m increases or ℓ decreases the ratio of $\omega_{c,min}/(\theta/t_f^2)$ will increase and the value of r will tend to be determined by minimum strength requirements with the resulting ω_c adequate to achieve fine motion control. When T_m decreases and ℓ increases the tendency will be for the ω_c resulting from r_{min} to be to low requiring $r > r_{min}$ for adequate fine motion control. These simple relations cannot predict where the limiting condition will change, only the tendency or relative change as the arm parameters change.

APPENDIX A

Analytical derivation of Frequency Functions

CASE 1: One Joint, Two Links

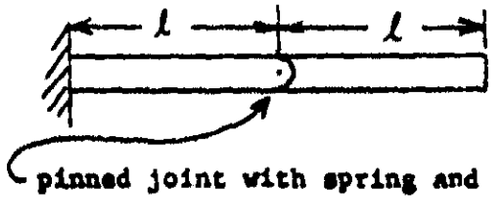

pinned joint with spring and dashpot

The relevant state variables at each point in the system

$-w$ = deflection perpendicular to the x axis

ψ = angle or slope of neutral axis with x axis

M = moment vector out of plane of vibration

V = shear in the direction of w

The relations between the state variables at each end of the two identical beam segments is given by the transfer matrix for a Bernoulli Euler beam.

$$\underline{z}_{left} = B\underline{z}_{right}$$

$$\begin{bmatrix} -w \\ \psi \\ M \\ V \end{bmatrix}_{left} = \begin{bmatrix} c_0 & \ell c_1 & a c_2 & a\ell c_3 \\ \beta^4 c_3/\ell & c_0 & a c_1/\ell & a c_2 \\ \beta^4 c_2/a & \beta^4 \ell c_3/a & c_0 & \ell c_1 \\ \beta^4 c_1/a\ell & \beta^4 c_2/a & \beta^4 c_3/\ell & c_0 \end{bmatrix} \begin{bmatrix} -w \\ \psi \\ M \\ V \end{bmatrix}_{right}$$

Where

$c_0 = (\cosh \beta + \cos \beta)/2$

$c_1 = (\sinh \beta + \sin \beta)/2$

$c_2 = (\cosh \beta - \cos \beta)/2\beta^2$

$c_3 = (\sinh \beta - \sin \beta)/2\beta^3$

$\beta^4 = \omega^2 \ell^4 \mu/EI$

$a = \ell^2/EI$

and μ = density/unit length

ω = circular frequency of vibration

E = Young's Modulus

I = cross sectional area moment of inertia

Across the joint $\underline{z}_{left} = K\ \underline{z}_{right}$

$$\begin{bmatrix} -w \\ \psi \\ M \\ V \end{bmatrix} = \begin{bmatrix} 1 & 0 & 0 & 0 \\ 0 & 1 & 1/k & 0 \\ 0 & 0 & 1 & 0 \\ 0 & 0 & 0 & 1 \end{bmatrix} \begin{bmatrix} -w \\ \psi \\ M \\ V \end{bmatrix}$$

left right

$k = k_R + j\omega c$

k_R = spring constant

c = damping coefficient

$j = \sqrt{-1}$

Let $\underline{z}_0$ = the state vector at the left end of the arm

$\underline{z}_1$ = the state vector at the right end of the arm

Then $\underline{z}_0 = B\ K\ B\ \underline{z}_1 = U\ \underline{z}_1$

if B describes the identical beam segments and K describes the spring loaded joint

Boundary Conditions require

$$\underline{z}_0 = \begin{bmatrix} -w_0 = 0 \\ \psi_0 = 0 \\ M_0 \\ V_0 \end{bmatrix} \qquad \underline{z}_1 = \begin{bmatrix} -w_1 \\ \psi_1 \\ M_1 = 0 \\ V_1 = 0 \end{bmatrix}$$

Thus the equation

$$\underline{z}_0 = U\,\underline{z}_1$$

Contains a homogeneous set of equations

$$-u_{11}\,w_1 + u_{12}\,\psi_1 = 0$$

$$-u_{21}\,w_1 + u_{22}\,\psi_2 = 0$$

For this always to be true the determinant of the submatrix of U must = 0 i.e.

$$\begin{vmatrix} u_{11} & u_{12} \\ u_{21} & u_{22} \end{vmatrix} = \underline{0}$$

All that is required is a great deal of algebraic manipulation and this requirement can be expressed in terms of the elements of the matrices A and K as follows:

$$-\sinh^2\beta\,(1 - 2\cos^2\beta) + \cos^2\beta + \frac{\beta\ell}{2ka}\,[\cos^2\beta \sinh\beta \cosh\beta - \cos\beta \sin\beta \cosh^2\beta\,] = 0$$

As $k_r \rightarrow \infty$ the expression

$$-\sinh^2\beta\,(1 - 2\cos^2\beta) + \cos^2\beta = 0$$

dominates. This is equivalent to expressions for single beams of length 2 ℓ.
As $k_r \rightarrow 0$, $c \rightarrow 0$

$$\cos^2\beta \sinh\beta \cosh\beta - \cos\beta \sin\beta \cosh^2\beta = 0$$

dominates and is equivalent to pinned beams without springs or dashpots.

Finally as EI becomes very large $\beta \rightarrow 0$, $a \rightarrow 0$ and via a series expansion of the trigonometric and hyperbolic function the frequency condition can be shown to converge to

$$\omega^2 - \frac{3k}{\mu\ell^3} = 0$$

Which is true for a simple second order system with inertia $\mu\ell^3/3$

CASE 2 :Two Joints, Two Links

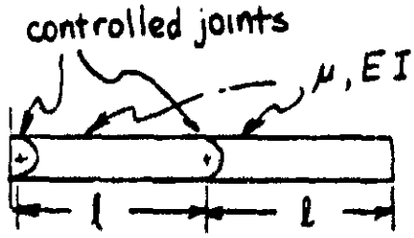

Now $U = K_1 B\, K_2 B$

which is equal to the transfer matrix in the one joint example premultiplied by K_1

Let us designate this as $U = K_1 D$
The frequency determinant requires evaluation of additional terms.

$$U = \begin{bmatrix} 1 & 0 & 0 & 0 \\ 0 & 1 & 1/k_1 & 0 \\ 0 & 0 & 1 & 0 \\ 0 & 0 & 0 & 1 \end{bmatrix} \begin{bmatrix} d_{11} & d_{12} & \text{---} \\ d_{21} & d_{22} & \text{---} \\ d_{31} & d_{32} & \text{---} \\ \text{---} & \text{---} & \text{---} \end{bmatrix}$$

The frequency determinant is

$$\begin{vmatrix} u_{11} & u_{12} \\ u_{21} & u_{22} \end{vmatrix} = \begin{vmatrix} d_{11} & d_{12} \\ d_{21} + \dfrac{d_{31}}{k_1} & d_{22} + \dfrac{d_{32}}{k_1} \end{vmatrix}$$

$$= \underbrace{d_{11}\, d_{22} - d_{12}\, d_{21}}_{\substack{\text{determinant for} \\ \text{the one joint case}}} + \frac{d_{11}\, d_{32}}{k_1} - \frac{d_{12}\, d_{31}}{k_1} = 0$$

requires only that d_{31} and d_{32} be evaluated since the detailed procedure for the one joint case would give d_{11} and d_{12} as

$$d_{11} = \cos^2\beta + \sinh^2\beta + \frac{\beta\ell}{4k_2a}(\sinh\beta + \sin\beta)(\cosh\beta - \cos\beta)$$

$$d_{12} = \frac{\ell}{\beta}(\cosh\beta \sinh\beta + \cos\beta \sin\beta) + \frac{\ell^2}{4k_2a}(\sinh^2\beta - \sin^2\beta)$$

The values of d_{31} and d_{32} are found by multiplication and simplification to be:

$$d_{31} = \frac{\beta^3\ell}{4ak_2}(\cosh\beta - \cos\beta)(\sinh\beta - \sin\beta) + \frac{\beta^2}{2a}(\cosh^2\beta - \cos^2\beta + \sinh^2\beta + \sin^2\beta)$$

$$d_{32} = \frac{\beta^2\ell^2}{4a^2k_2}(\sinh\beta - \sin\beta)^2 + \frac{\beta\ell}{a}(\cosh\beta \sinh\beta - \cos\beta \sin\beta)$$

These expressions, or values obtained from them, can then be fed into the frequency determinant.

APPENDIX B

Rigid Body Analysis of Two-Link Two-Joint Case

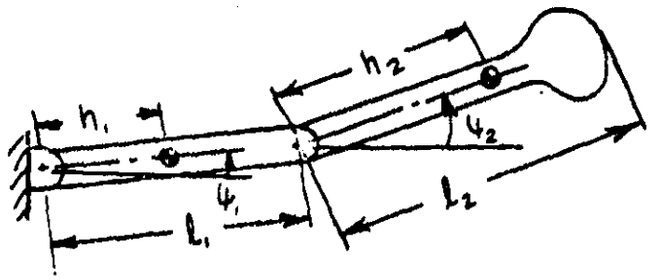

I_1 = mass moment of Inertia about c.g. of link 1

I_2 = mass moment of Inertia about c.g. of link 2

m_1, m_2 mass of links 1 and 2

Two Link Two Joint Arm

The kinetic energy of the system for small angles ψ_1 and ψ_2

$$T = \frac{1}{2} \left[(I_1 + m_1 h_1^2 + m_2 \ell_1^2)\dot{\psi}_1^2 + (I_2 + h_2^2 m_2)\dot{\psi}_2^2 + 2h_2 \ell_1 m_2 \dot{\psi}_1 \dot{\psi}_2 \right]$$

The potential energy (with no gravity) with rotary springs of constant k_1 and k_2 at the joints

$$V = \frac{1}{2} \left[k_1 \psi_1^2 + k_2 (\psi_2 - \psi_1)^2 \right]$$

Lagrange's equations require for i = 1,2 that

$$\frac{d}{dt} \left[\frac{\partial}{\partial \dot{\psi}_i} (T - V) \right] - \frac{\partial}{\partial \psi_1} (T - V) = 0$$

For the homogeneous solution to linear differential equations

$$\ddot{\psi}_i = -\omega^2 \psi_i$$

where ω = frequency of vibration in radians/sec.

Computing the appropriate derivatives and arranging the results in matrix form yields:

$$\text{(B1)} \begin{bmatrix} k_1+k_2-(I_1+m_1h_1^2+m_2\ell_1^2)\omega^2 & -k_2h_2\ell_1m_2\omega^2 \\ -k_2-h_2\ell_1m_2\omega^2 & k_2-(I_2+h_2^2m_2)\omega^2 \end{bmatrix} \begin{bmatrix} \psi_1 \\ \psi_2 \end{bmatrix} = \begin{bmatrix} 0 \\ 0 \end{bmatrix}$$

The determinant of the 4 x 4 matrix must be zero, which gives a condition for determining the natural frequencies ω.

Equal Links

If the two links are identical (B1) simplifies to

$$\text{(B2)} \begin{bmatrix} k_1+k_2-4m\ell^2\omega^2/3 & -k_2-\ell^2m\omega^2/2 \\ -k_2-\ell^2m\omega^2/2 & k_2-m\ell^2\omega^2/3 \end{bmatrix} \begin{bmatrix} \psi_1 \\ \psi_2 \end{bmatrix} = \begin{bmatrix} 0 \\ 0 \end{bmatrix}$$

where $\ell = \ell_1 = \ell_2$, $m = m_1 = m_2$ $\quad I_1 = I_2 = m\ell_2/3$

which expands and simplifies to

$$\text{(B3)} \quad k_1k_2 - \frac{m\ell^2}{3}\omega^2(k_1+8k_2) + \frac{7}{36}m^2\ell^4\omega^4 = 0$$

Equation (B3) will be used to obtain natural frequencies in both the damped and undamped cases.

Undamped Natural Frequencies

If we make the substitution of variables into equation(B3)

$$q^2 = \frac{m \ell^2 \omega^2}{3 k_2}$$

and divide by k_2^2 we obtain

(B4) $$\frac{k_1}{k_2} - \left(\frac{k_1}{k_2} + 8\right) q^2 + \frac{7}{4} q^4 = 0$$

The variable q corresponds to the natural frequency with the inboard joint clamped. The solution of (B4) yields two roots which are a nondimensionalized form of the natural frequencies of the original problem.

Damped Natural Frequencies (complex)

The damped case can be obtained directly from equation (B3) by a change in notation.

$$k_1 \Longrightarrow k_1 + j\omega c_1$$
$$k_2 \Longrightarrow k_2 + j\omega c_2$$

and $s = j\omega \qquad I = m\ell^2/3$

The characteristic equation for determining the values of s is

$$7s^4/4 + s^3 I(c_1 + 8c_2) + s^2[I(k_1 + 8k_2) - c_1c_2] + s(k_1c_2 + k_2c_1) + k_1k_2 = 0$$

Figure 1. State Vector for Arm Models

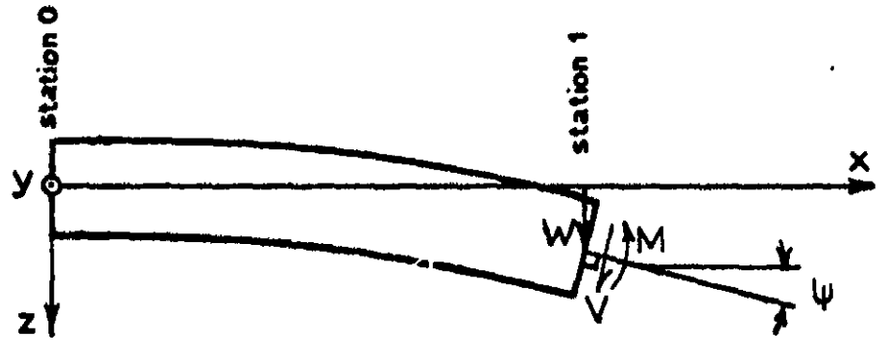

$$Z_1 = \begin{bmatrix} -W \\ \psi \\ M \\ V \end{bmatrix}_1 = \begin{bmatrix} -\text{displacement} \\ \text{angle} \\ \text{moment} \\ \text{shear force} \end{bmatrix}_{\text{at station 1}}$$

$$Z_0 = B Z_1$$

B = beam transfer matrix

Figure 2.Transfer Matrix Representation of an Arm

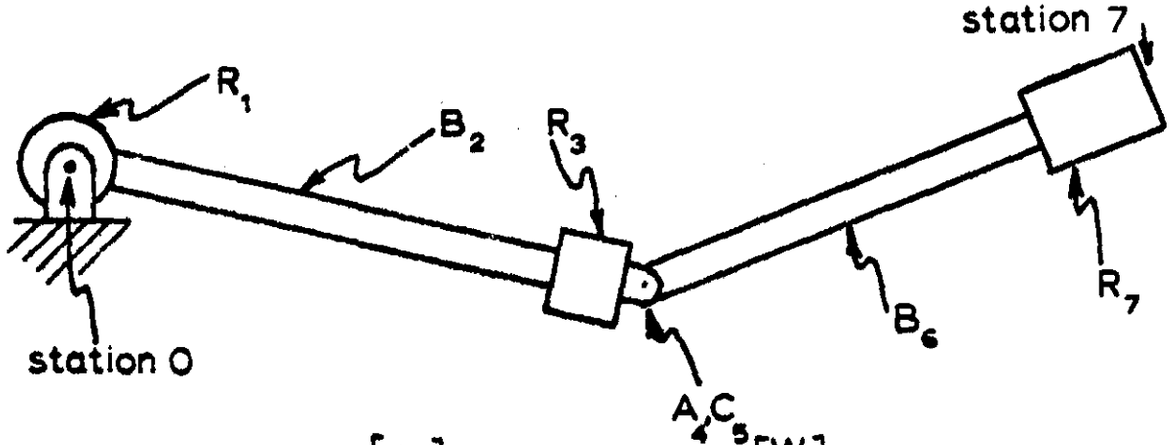

$$\begin{bmatrix} -W \\ \psi \\ M \\ V \end{bmatrix}_0 = R_1 B_2 R_3 A_4 C_5 B_6 R_7 \begin{bmatrix} W \\ \psi \\ M \\ V \end{bmatrix}_7$$

Figure 3a. Distributed Beam Transfer Matrix

Distributed Beam Transfer Matrix (Timoshenko model)

$$B = \begin{bmatrix} c_0 - \sigma c_2 & l[c_1 - (\sigma+\tau)c_3] & ac_2 & \frac{al}{\beta^4}[-\sigma c_1 + (\beta^4+\sigma^2)c_3] \\ \frac{\beta^4}{l} c_3 & c_0 - \tau c_2 & \frac{a}{l}(c_1 - \tau c_3) & ac_2 \\ \frac{\beta^4}{a} c_2 & \frac{l}{a}[-\tau c_1 + (\beta^4+\tau^2)c_3] & c_0 - \tau c_2 & l[c_1 - (\sigma+\tau)c_3] \\ \frac{\beta^4}{al}(c_1 - \sigma c_3) & \frac{\beta^4}{a} c_2 & \frac{\beta^4}{l} c_3 & c_0 - \sigma c_2 \end{bmatrix}$$

where

$$a = \frac{l^2}{EJ} \qquad c_0 = A(\lambda_2^2 \cosh \lambda_1 + \lambda_1^2 \cos \lambda_2)$$

$$\beta^4 = \frac{\mu\omega^2}{EJ} l^4 \qquad c_1 = A\left(\frac{\lambda_2^2}{\lambda_1} \sinh \lambda_1 + \frac{\lambda_1^2}{\lambda_2} \sin \lambda_2\right)$$

$$\sigma = \frac{\mu\omega^2}{GA_s} l^2 \qquad c_2 = A(\cosh \lambda_1 - \cos \lambda_2)$$

$$\tau = -\frac{l^2}{EJ}(\mu i^2 \omega^2) \qquad c_3 = A\left(\frac{1}{\lambda_1} \sinh \lambda_1 - \frac{1}{\lambda_2} \sin \lambda_2\right)$$

$$\lambda_{\frac{1}{2}} = +\sqrt{\sqrt{\beta^4 + \tfrac{1}{4}(\sigma-\tau)^2} \mp \tfrac{1}{2}(\sigma+\tau)} \qquad A = \frac{1}{\lambda_1^2 + \lambda_2^2}$$

GA_s = Shear stiffness

EJ = Bending stiffness

μ = Mass per unit length

i = Radius of gyration of cross sectional area perpendicular to the beam's neutral axis

l = length of the beam

ω = vibration circular frequency

Figure 3b. Angle Transfer Matrix

$$A = \begin{bmatrix} 1/\cos\phi & 0 & 0 & 0 \\ 0 & 1 & 0 & 0 \\ 0 & 0 & 1 & 0 \\ m_s\omega^2 \sin\phi \tan\phi & 0 & 0 & \cos\phi \end{bmatrix}$$

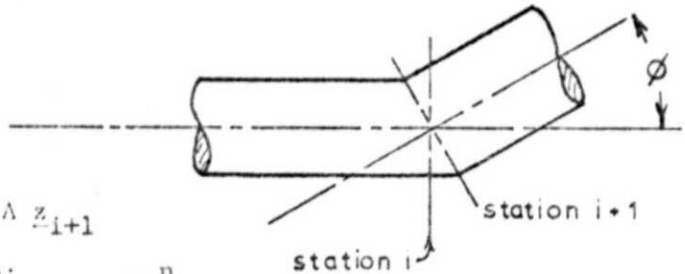

$\underline{z}_i = A\,\underline{z}_{i+1}$

where:

$$m_s = \sum_{j=i}^{n} m_j$$

m_j = mass of element j

n = first joint (angle) element greater than i, or the total number of elements, whichever is smaller

ω = vibration circular frequency

Figure 3c. Rigid Mass Transfer Matrix

$$R = \begin{bmatrix} 1 & \ell & 0 & 0 \\ 0 & 1 & 0 & 0 \\ m\omega^2(\ell - h) & I_g\omega^2 + m\omega^2(\ell - h) & 1 & \ell \\ m\omega^2 & m\omega^2(\ell - h) & 0 & 1 \end{bmatrix}$$

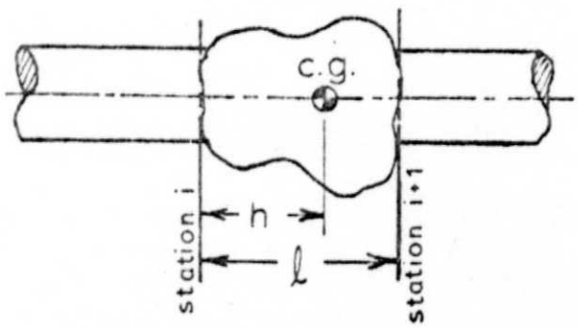

$\underline{z}_i = R\,\underline{z}_{i+1}$

I_g = mass moment of inertia, axis perpendicular to the plane of vibration, through the center of gravity, c.g.

m = mass of the body

ω = vibration circular frequency

Figure 3d Controlled Rotary Joint Transfer Matrix

$$C = \begin{bmatrix} 1 & 0 & 0 & 0 \\ 0 & 1 & 1/k(j\omega) & 0 \\ 0 & 0 & 1 & 0 \\ 0 & 0 & 0 & 1 \end{bmatrix}$$

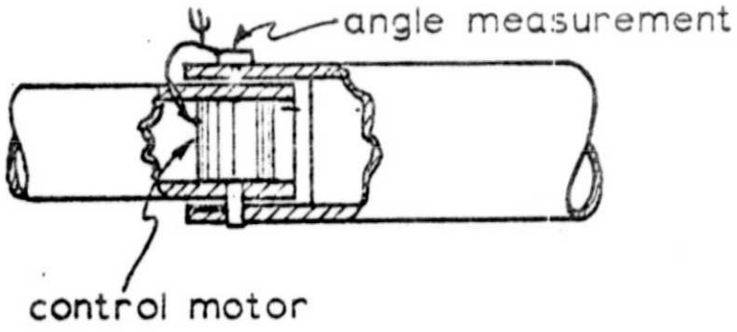

Pinned connection between two elements. Relative angle is related to the moment which affects each of the two elements. $k(j\omega)$ is essentially the transfer function relating moment to angle. In the simplest case k = constant a rotary spring determines the relation between angle and moment, $k(j\omega)$ can account for feedback of angular velocity and other derivatives or integrals of the variable Ψ, for filter dynamics included for compensation, and for servo motor and transmission dynamics.

Figure 4. Physically Possible Boundary Conditions

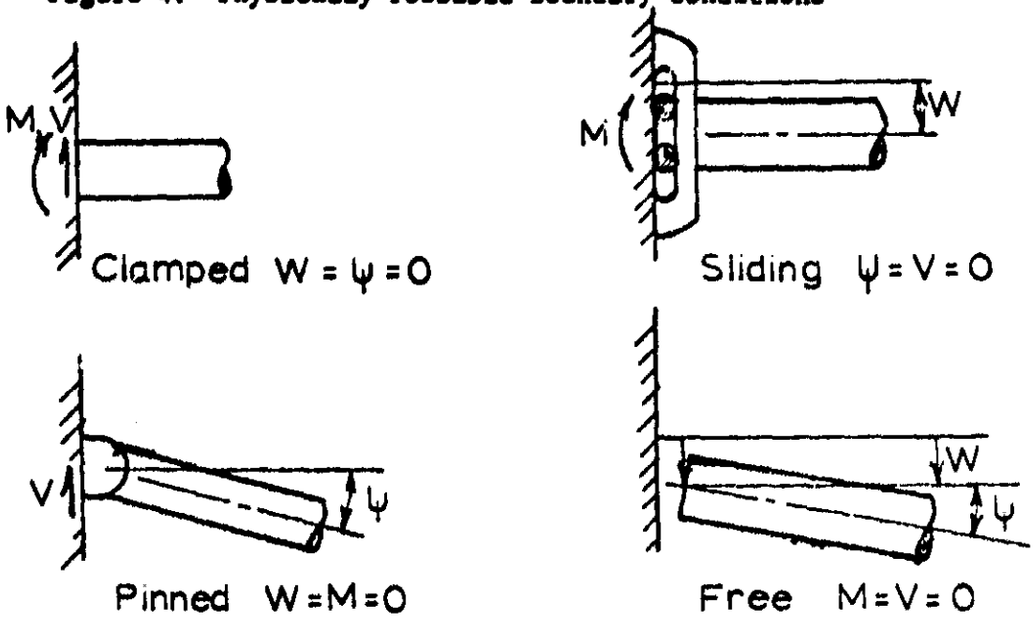

Figure 5. Frequency Determinant

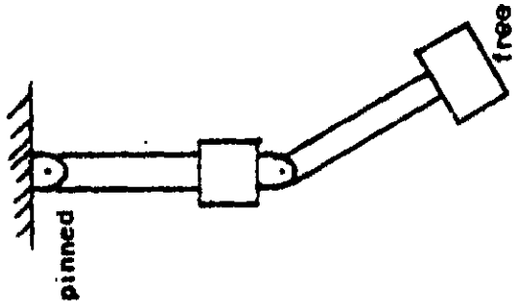

$$U = B_1 R_2 A_3 C_4 B_5 R_6$$

$$z_0 = \begin{bmatrix} -W \\ \psi \\ M \\ V \end{bmatrix}_0 = \begin{bmatrix} u_{11} & u_{12} & u_{13} & u_{14} \\ u_{21} & u_{22} & u_{23} & u_{24} \\ u_{31} & u_{32} & u_{33} & u_{34} \\ u_{41} & u_{42} & u_{43} & u_{44} \end{bmatrix} \begin{bmatrix} -W \\ \psi \\ M \\ V \end{bmatrix}_6 \quad \begin{matrix} 0 \\ \\ 0 \\ 0 \end{matrix}$$

$$\begin{bmatrix} u_{11} & u_{12} \\ u_{31} & u_{32} \end{bmatrix} \begin{bmatrix} W \\ \psi \end{bmatrix}_6 = \begin{bmatrix} 0 \\ 0 \end{bmatrix}$$

For a nontrivial solution:

$$u_{11} u_{32} - u_{12} u_{31} = 0$$

Figure 6 Experimental Verification - Clamped elbow joint

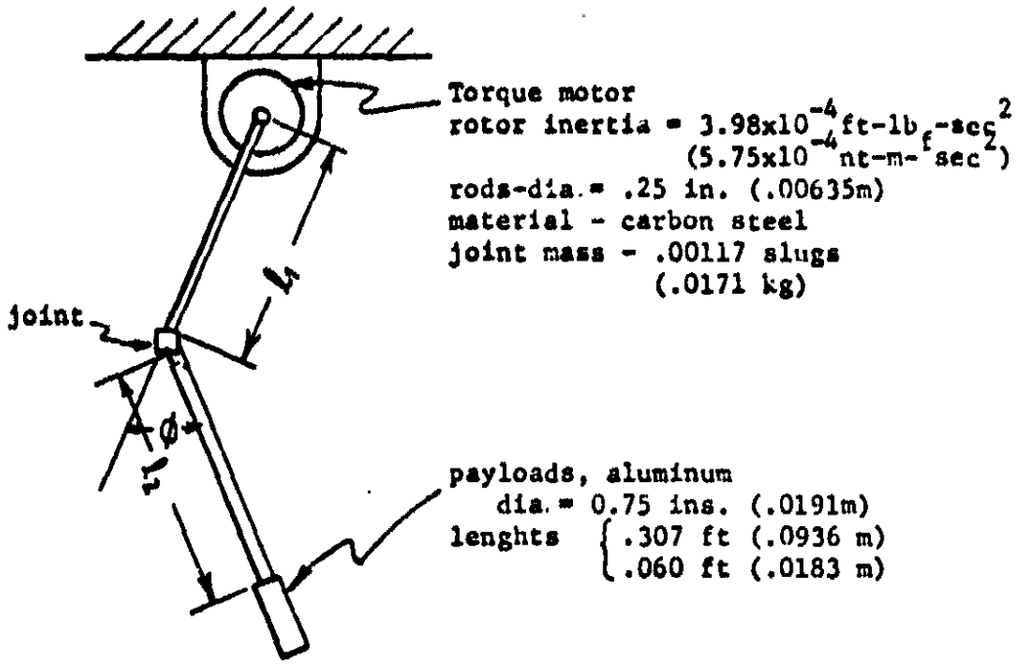

Figure 7 Experimental Verification -pinned elbow joint

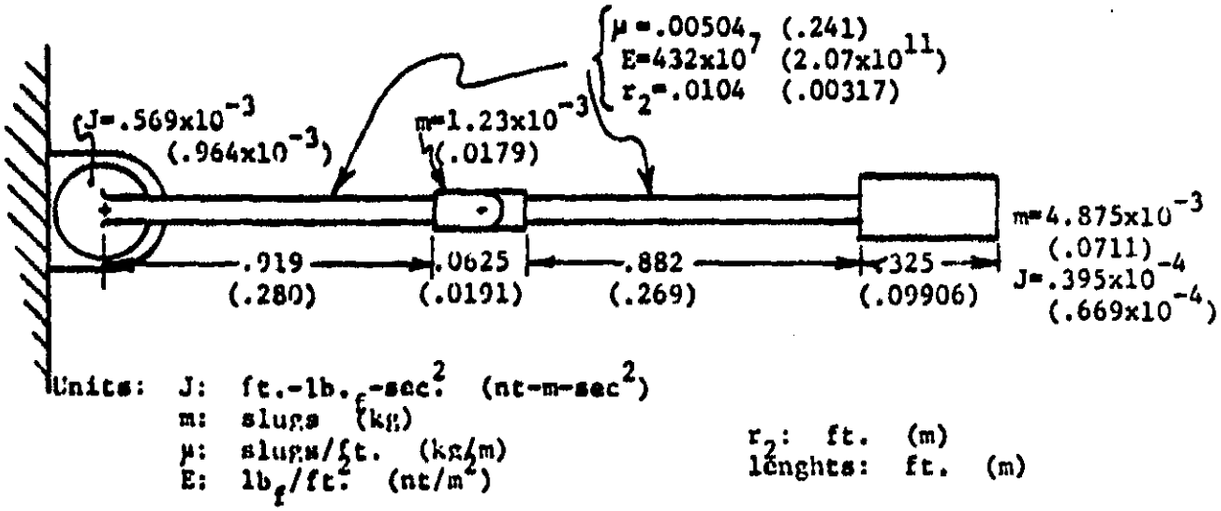

Figure 8. Amplitude of Acceleration vs. Frequency

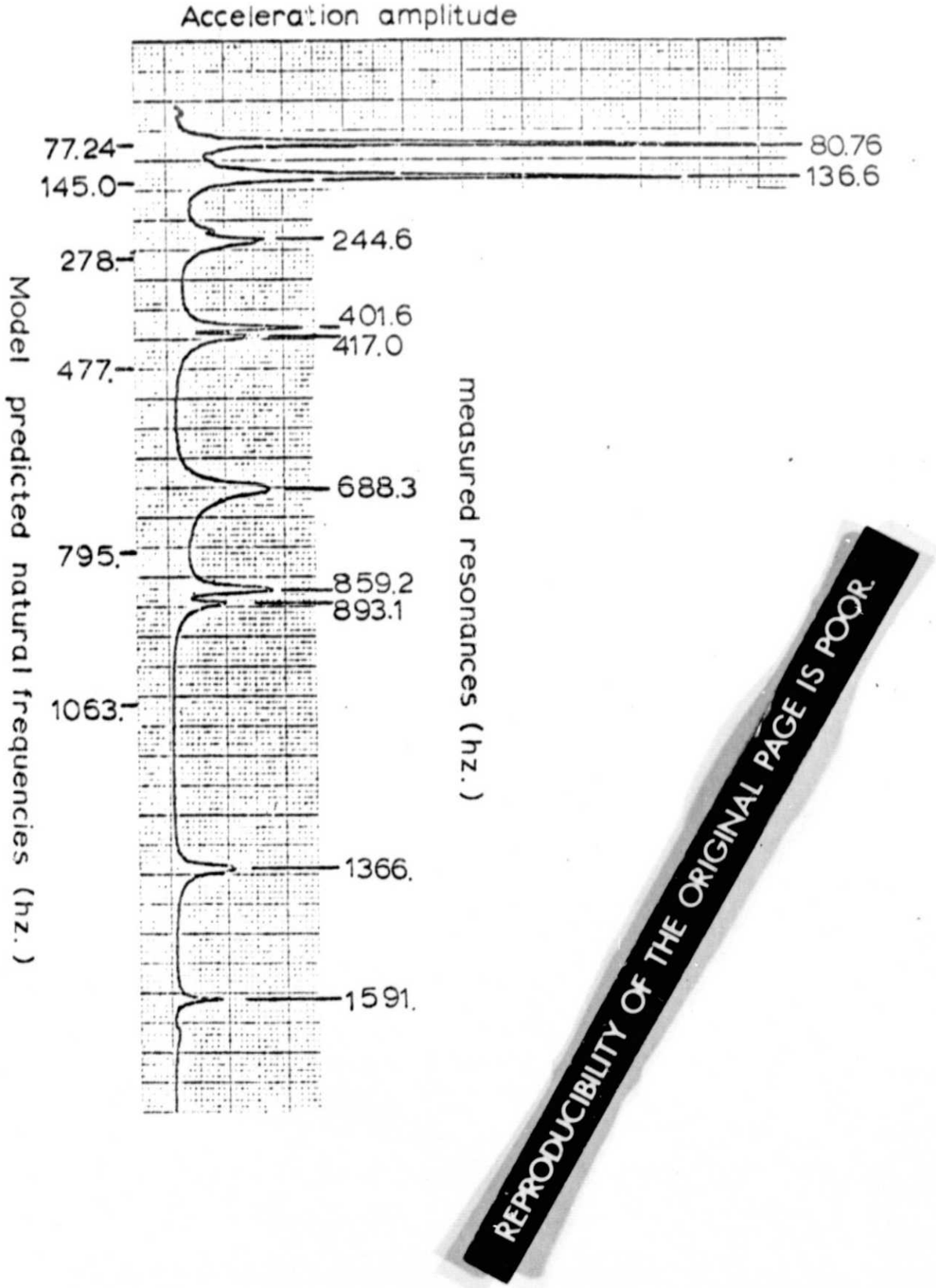

Figure 9. One Joint, Two Link Arm Example

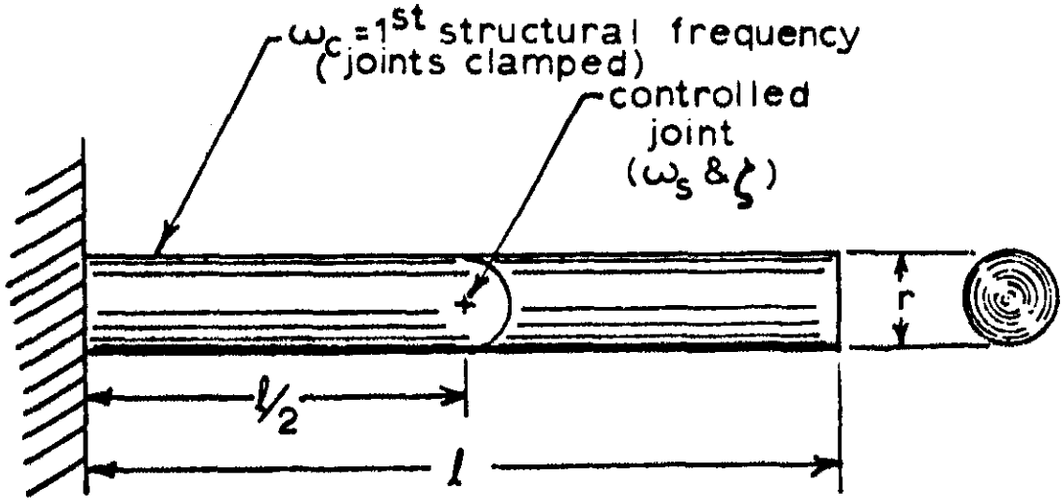

Figure 10. Three Characteristic Root Loci. Each plot indicates the position of the three dominant roots of the arm of Figure 9 for different servo bandwidth. Arrows indicate direction of root movement for increasing values of damping ratio.

a. Rigid Region ($\bar{\omega}_s << .386$)
Characteristic second order system for reasonable values of damping. Figure 11a for detail.

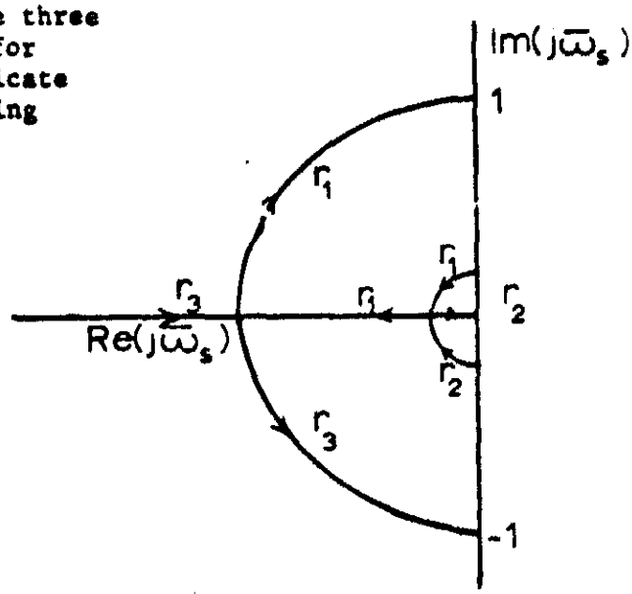

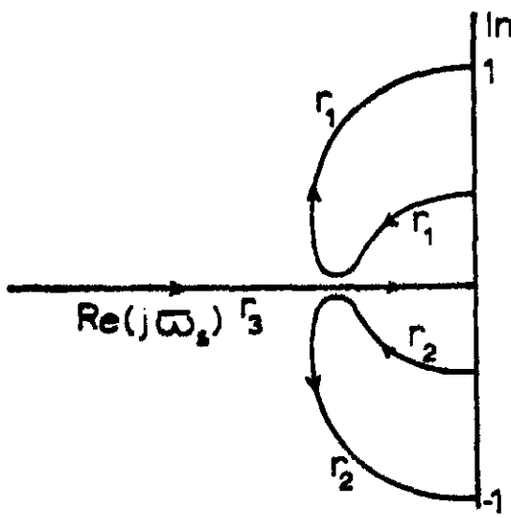

b. Transition Region. ($\bar{\omega}_s \approx 0.386$)
A triple root occurs at the critical value of $\omega_s = 0.386$ for $\zeta = .915$.
Figure 11b for detail.

c. Floppy Region. ($\bar{\omega}_s >> 0.386$)
It is no longer possible to bring the dominant complex roots near the real axis. Figure 11c for detail.

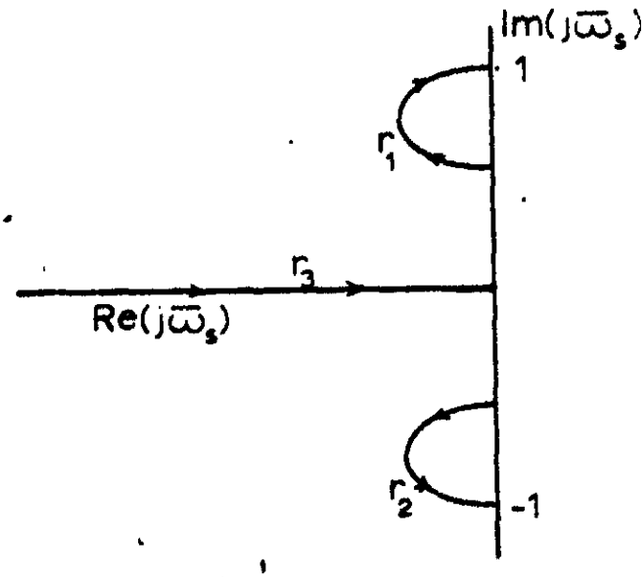

Figure 11a. Detail Root Loci of Dominant Roots.
Varying ζ, ω_s/ω_c=0.167

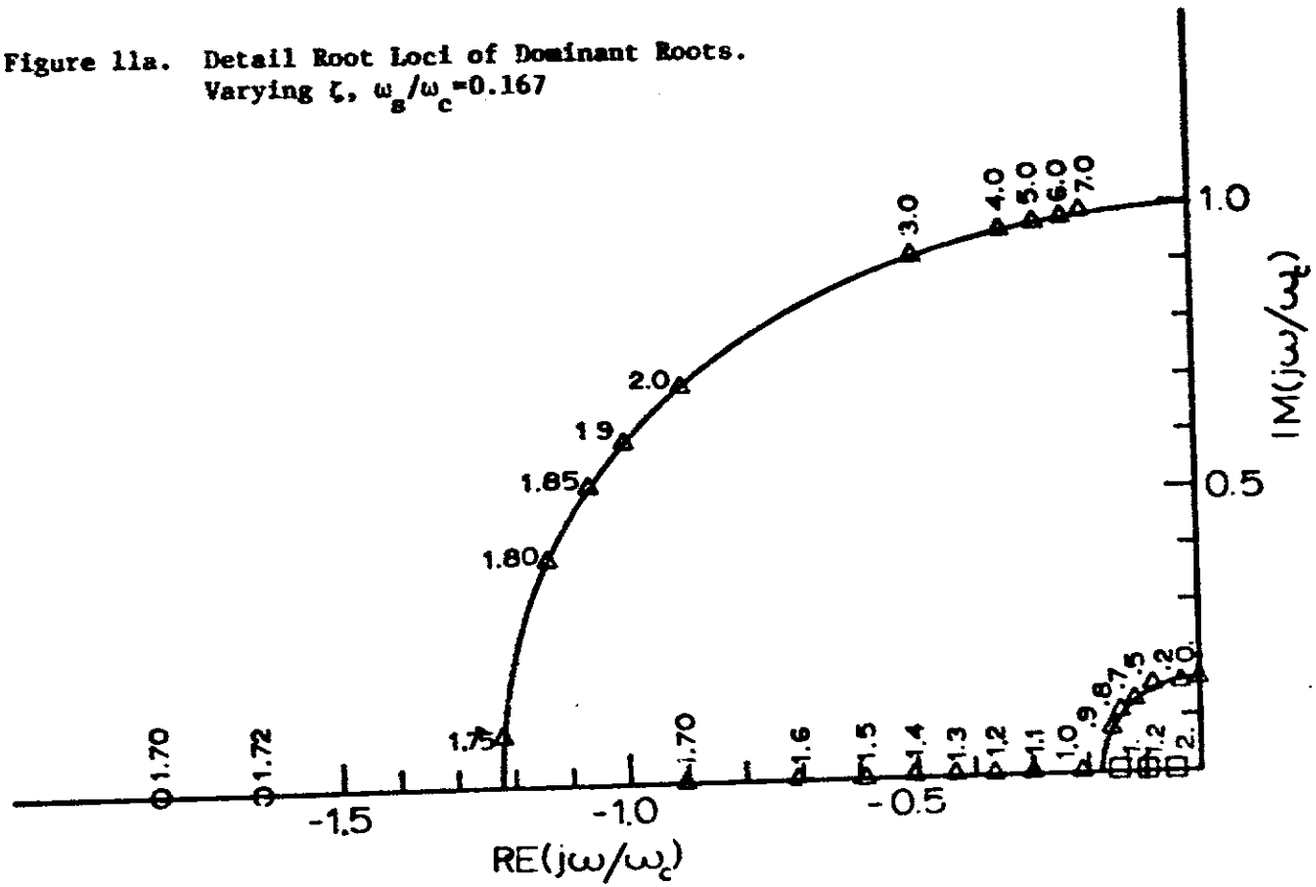

Figure 11b. Detail Root Loci of Dominant Roots.
Varying ζ, ω_s/ω_c=0.383

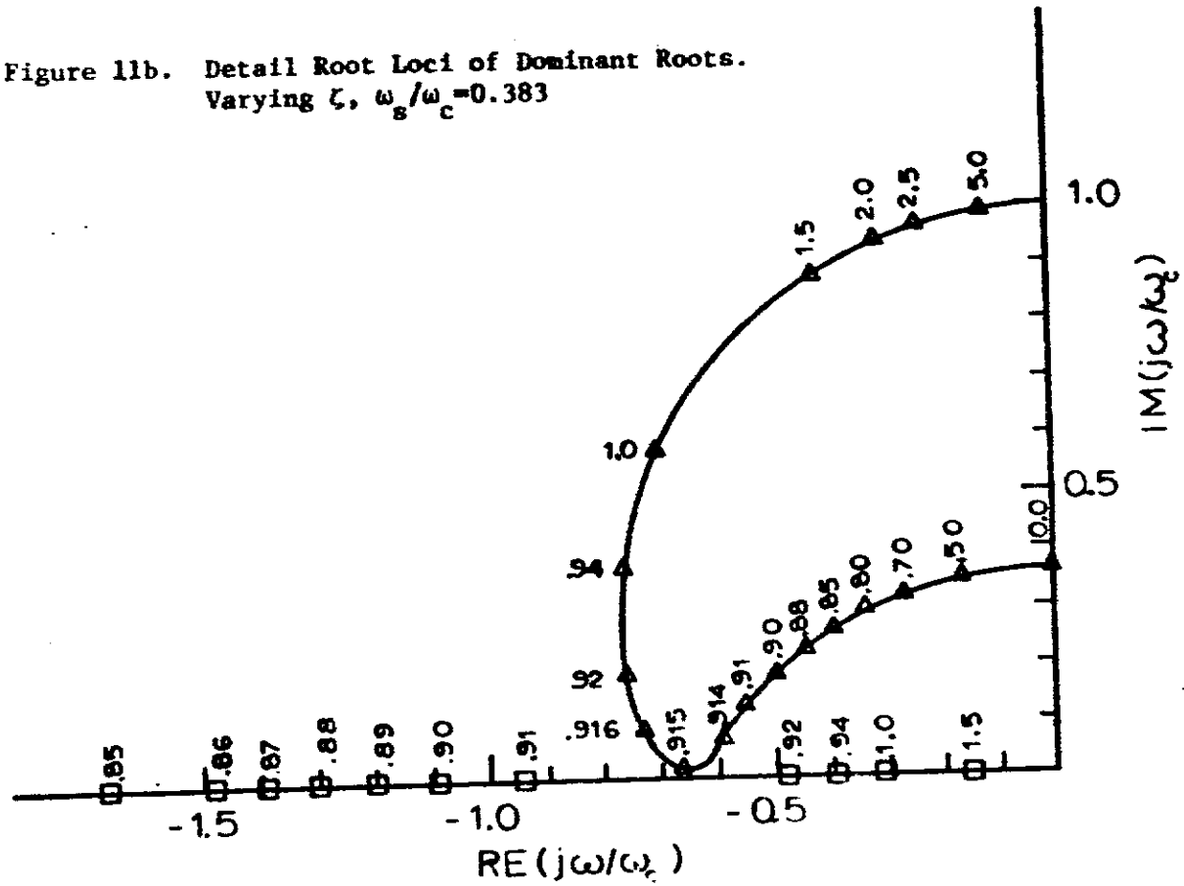

Figure 11c. Detail Root Loci of Dominant Roots.
Varying ζ, ω_s/ω_c=0.50

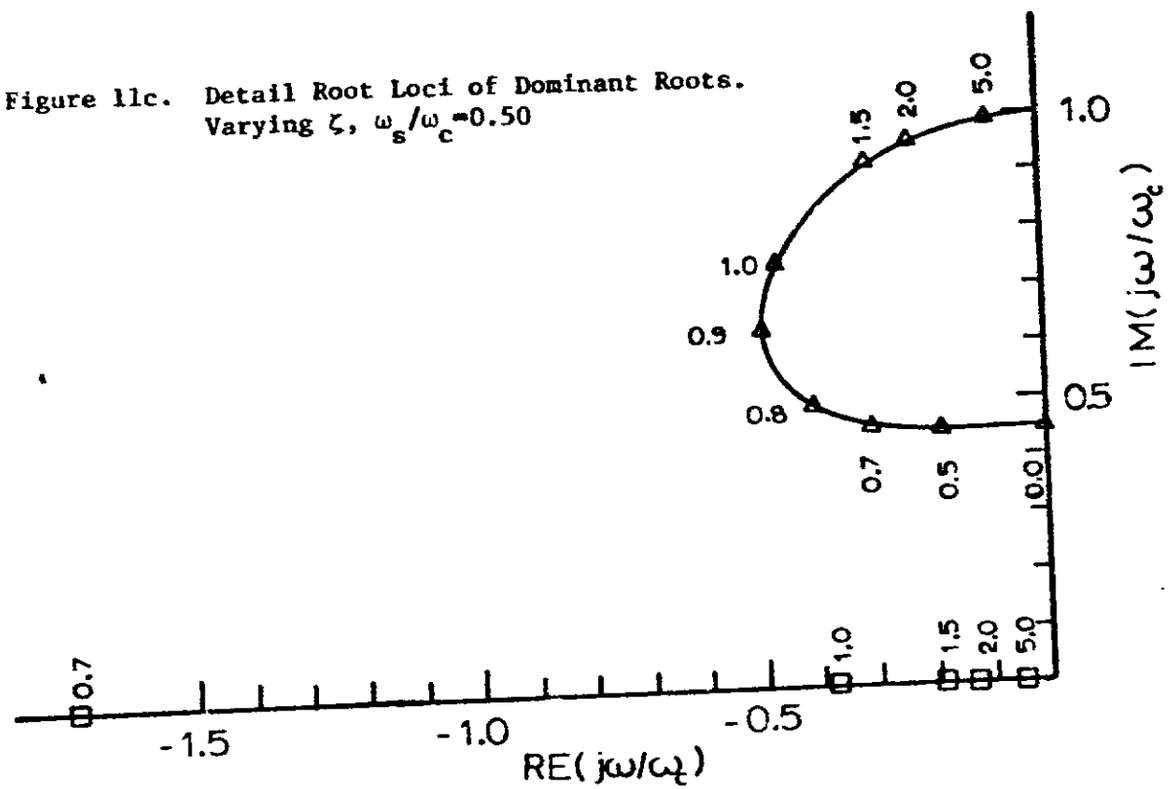

Figure d. Summary of Complex Root Loci

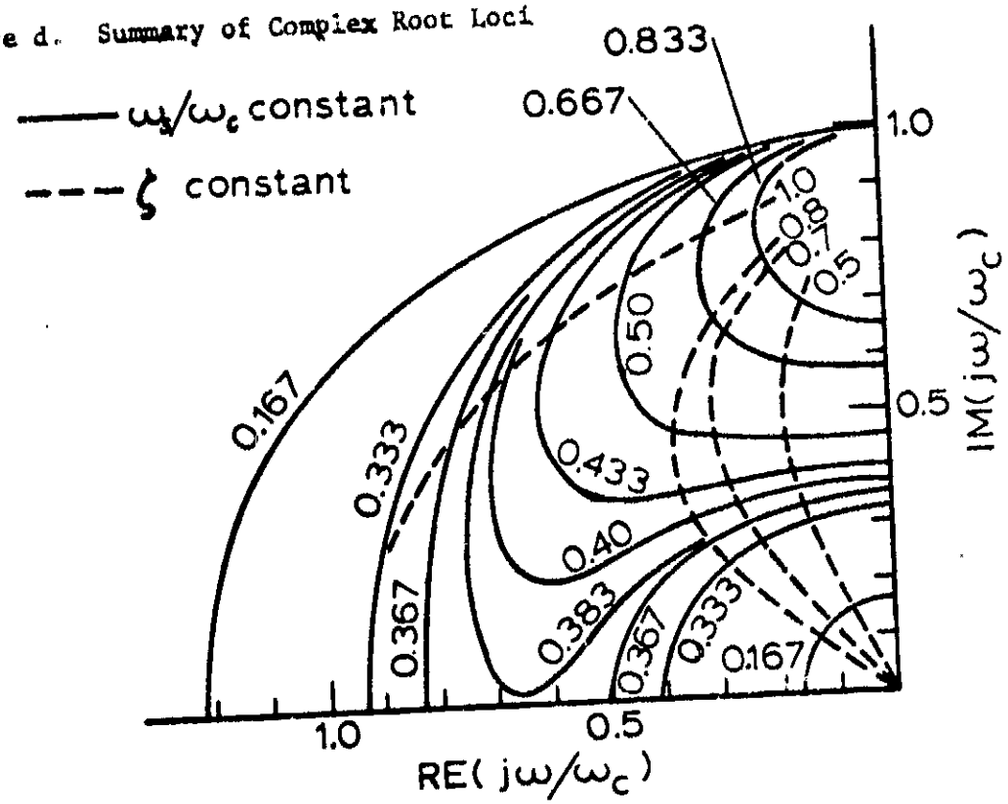

Figure 12. Higher Order Root Loci Varying ζ.

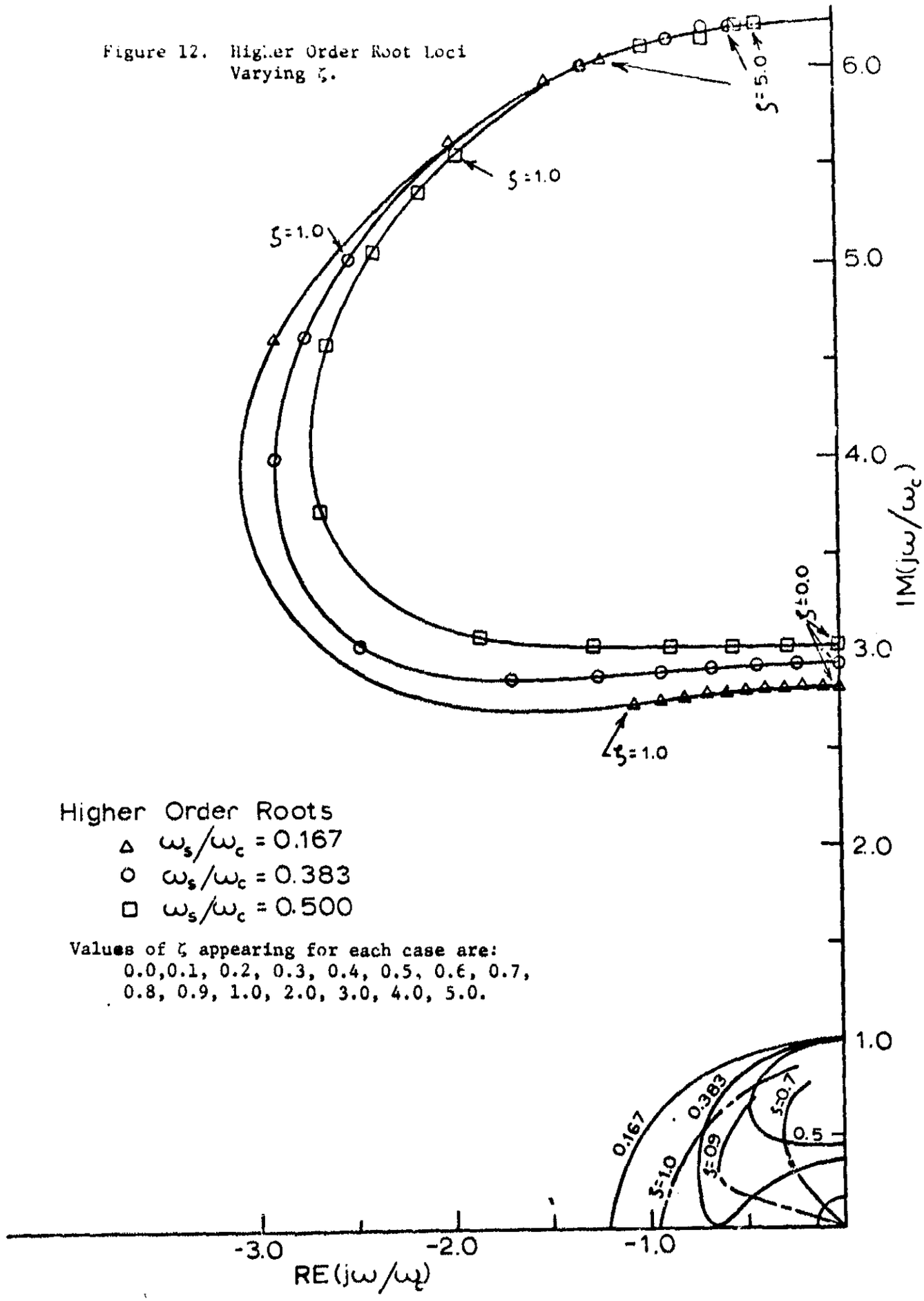

Figure 13. System Roots for Optimal Fourth Order Systems by Various Criteria

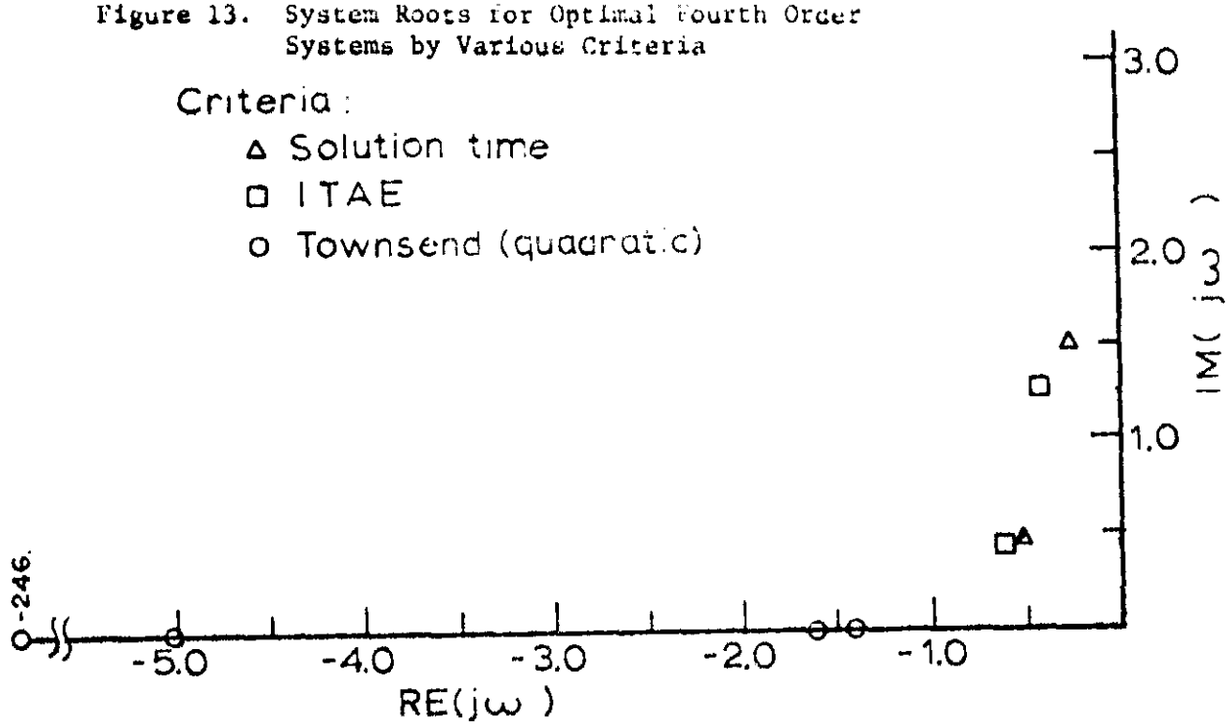

Figure 14. Root Nomenclature Indicated on Four Undamped Roots.
(r_2*=Complex Conjugate of r_2)

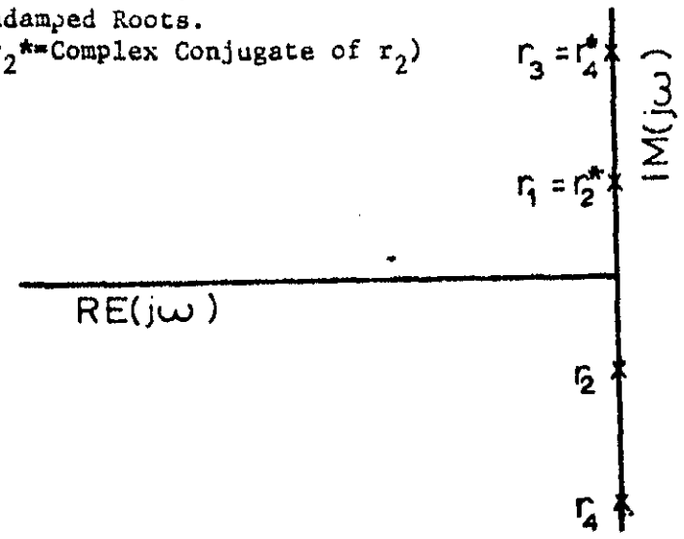

Figure 15a. Undamped Natural Frequencies for a Rigid Two Joint Arm. Nondimensionalized with respect to a one joint (elbow) arm with same feedback gains. Plotted versus ratio of position feedback gains.

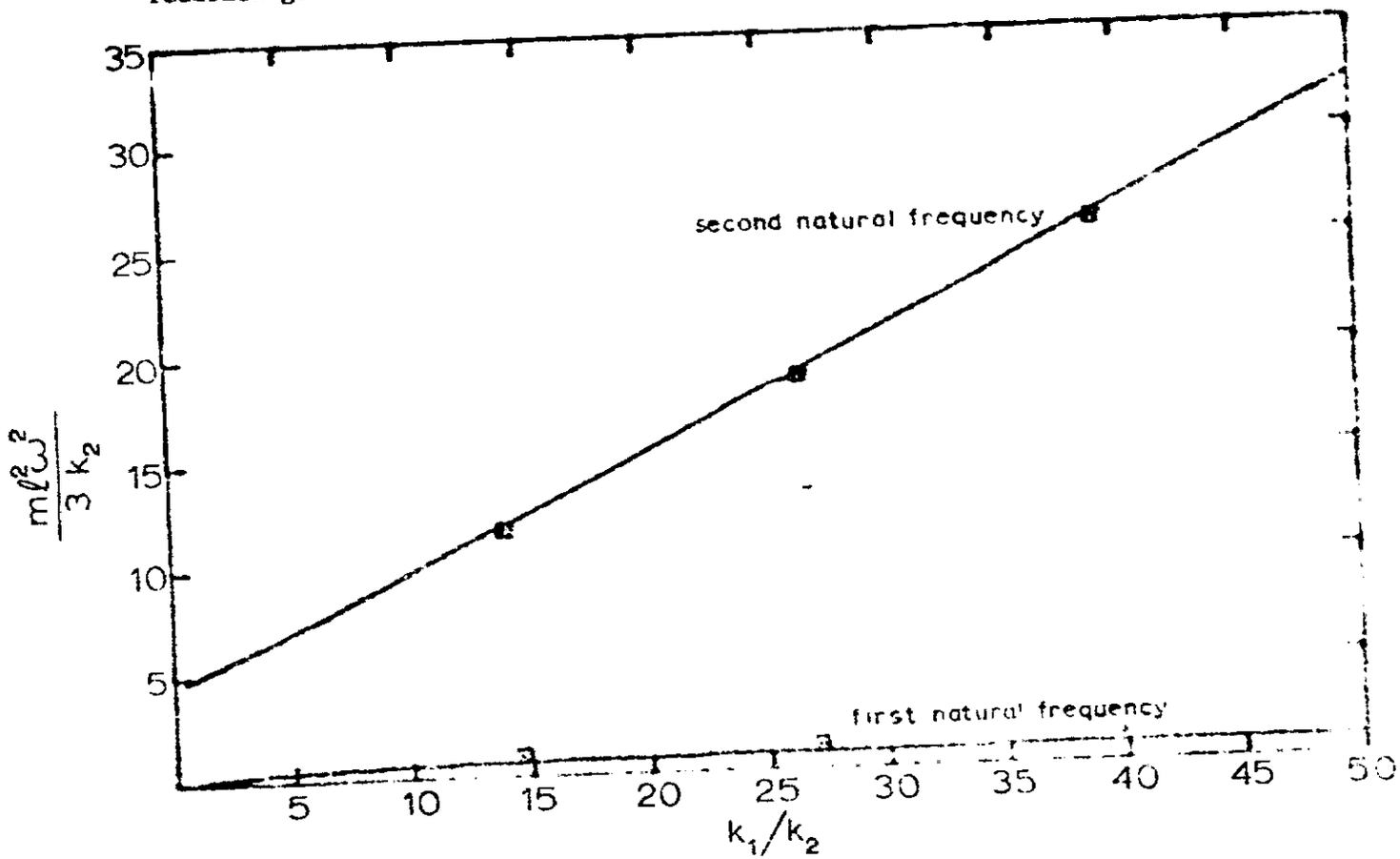

Figure 15b. First Undamped Natural Frequency for a Rigid Two Join Arm. (Expanded Scale)

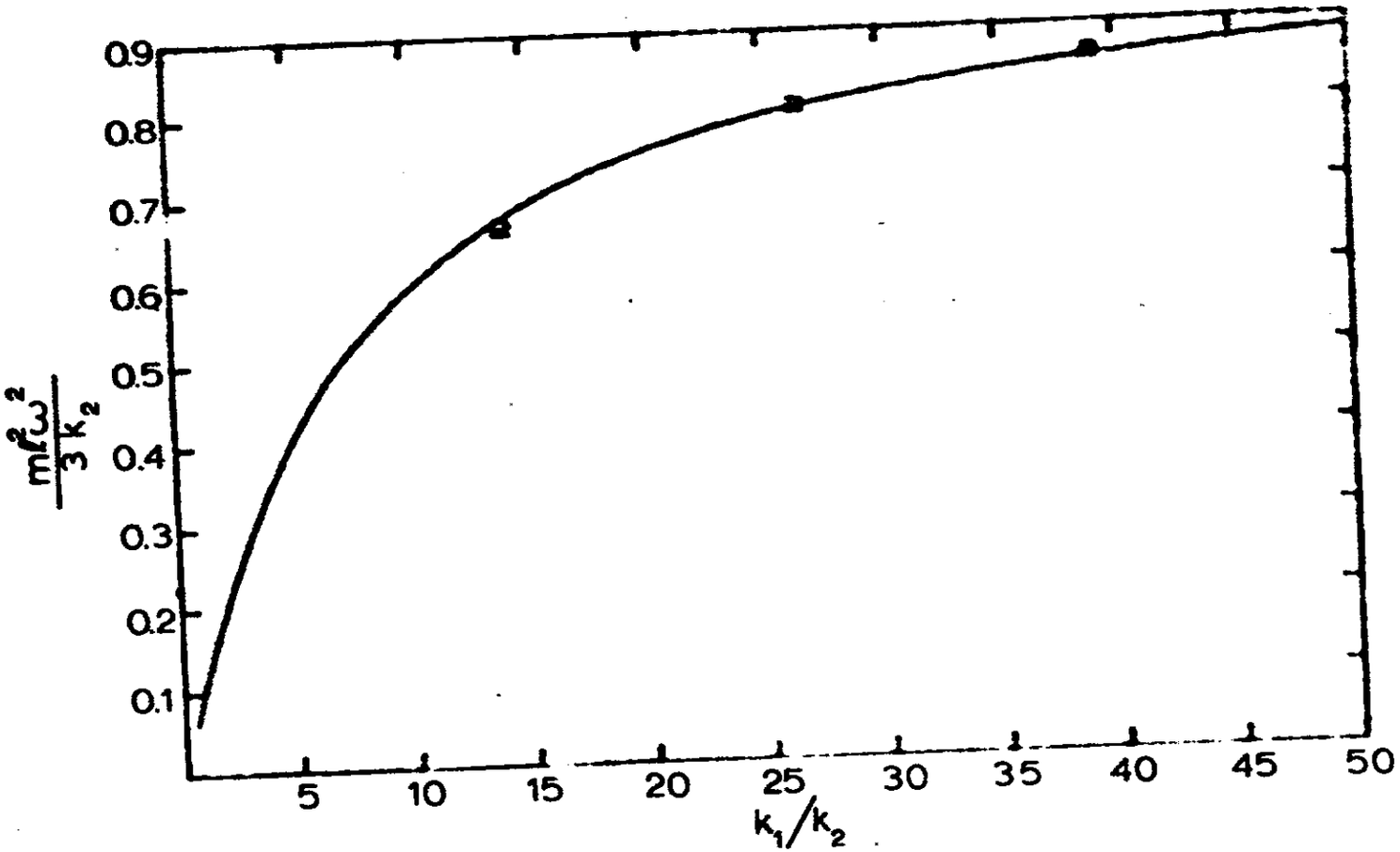

Figure 16a. Root Loci of Nondimensional Rigid Two Joint Arm: $k_1=2$.

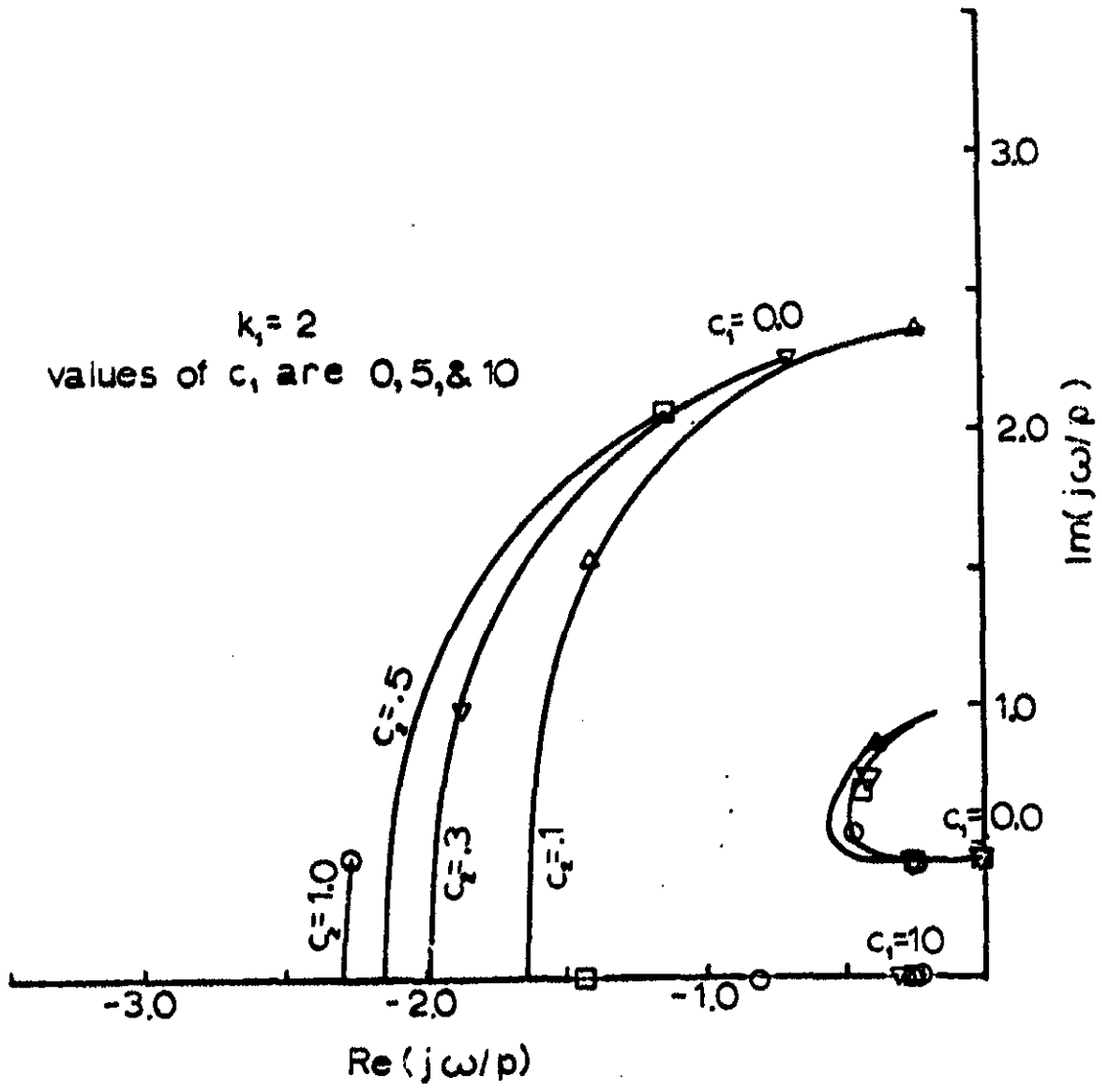

Figure 16b. Root Loci of Nondimensional Rigid Two Joint Arm: $k_1=5$

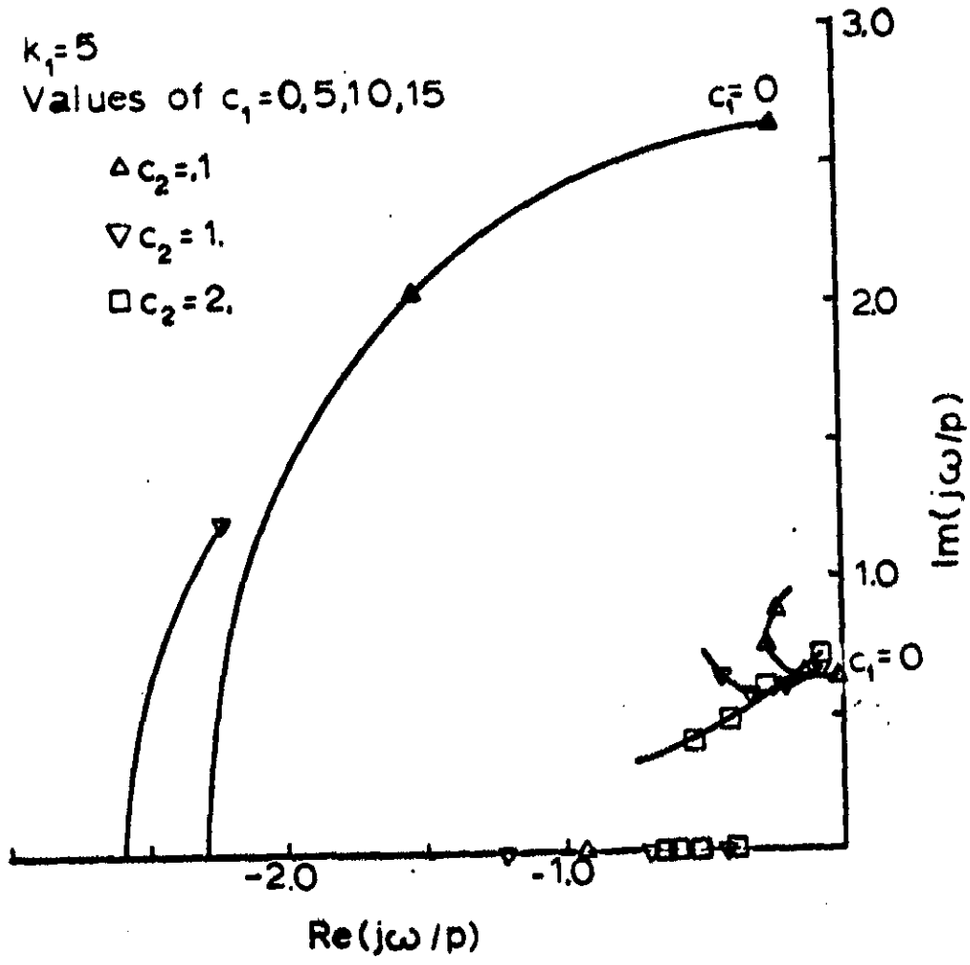

Figure 16c. Root Loci of Nondimensional Rigid Two Joint Arm: k_1=10

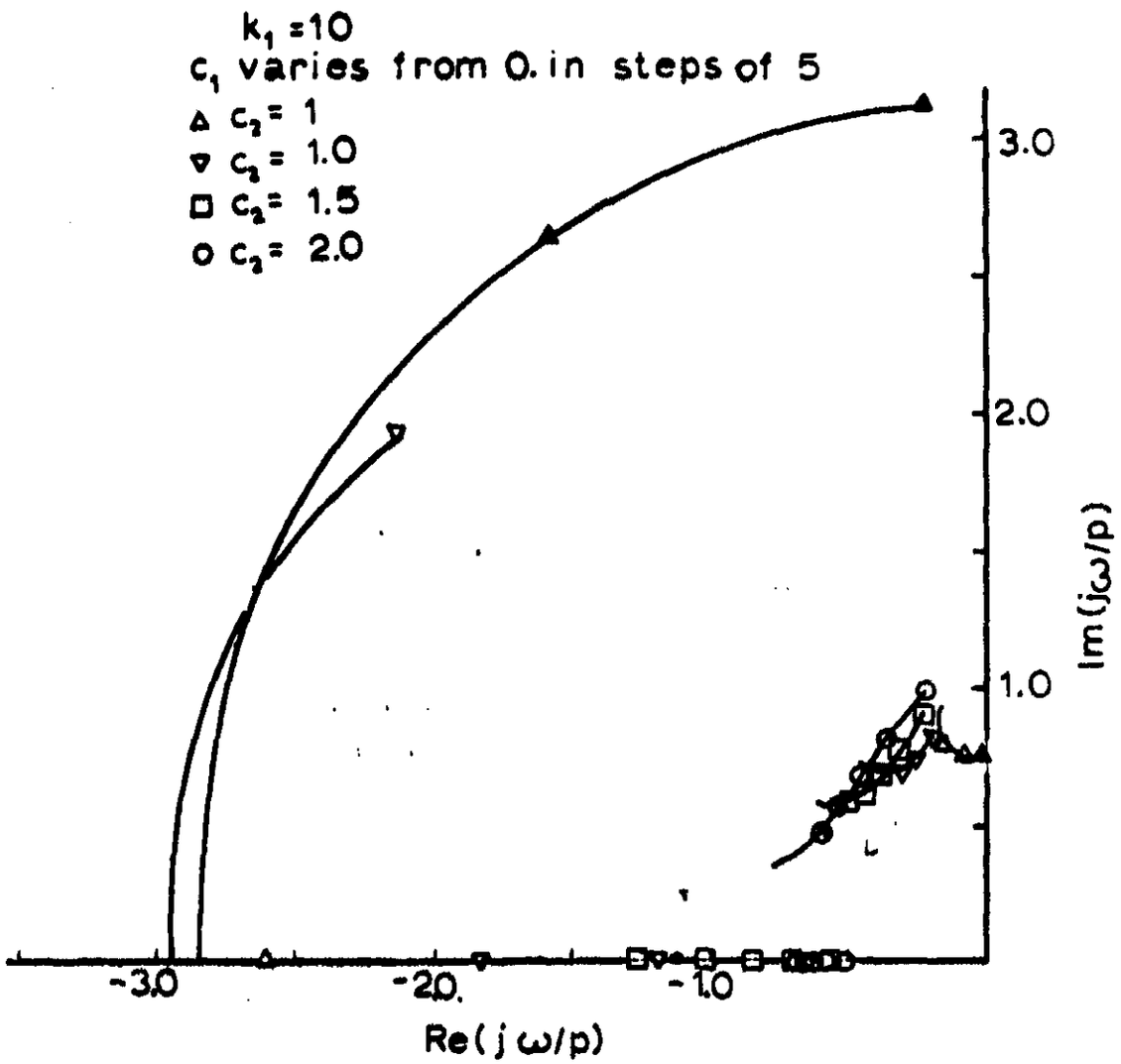

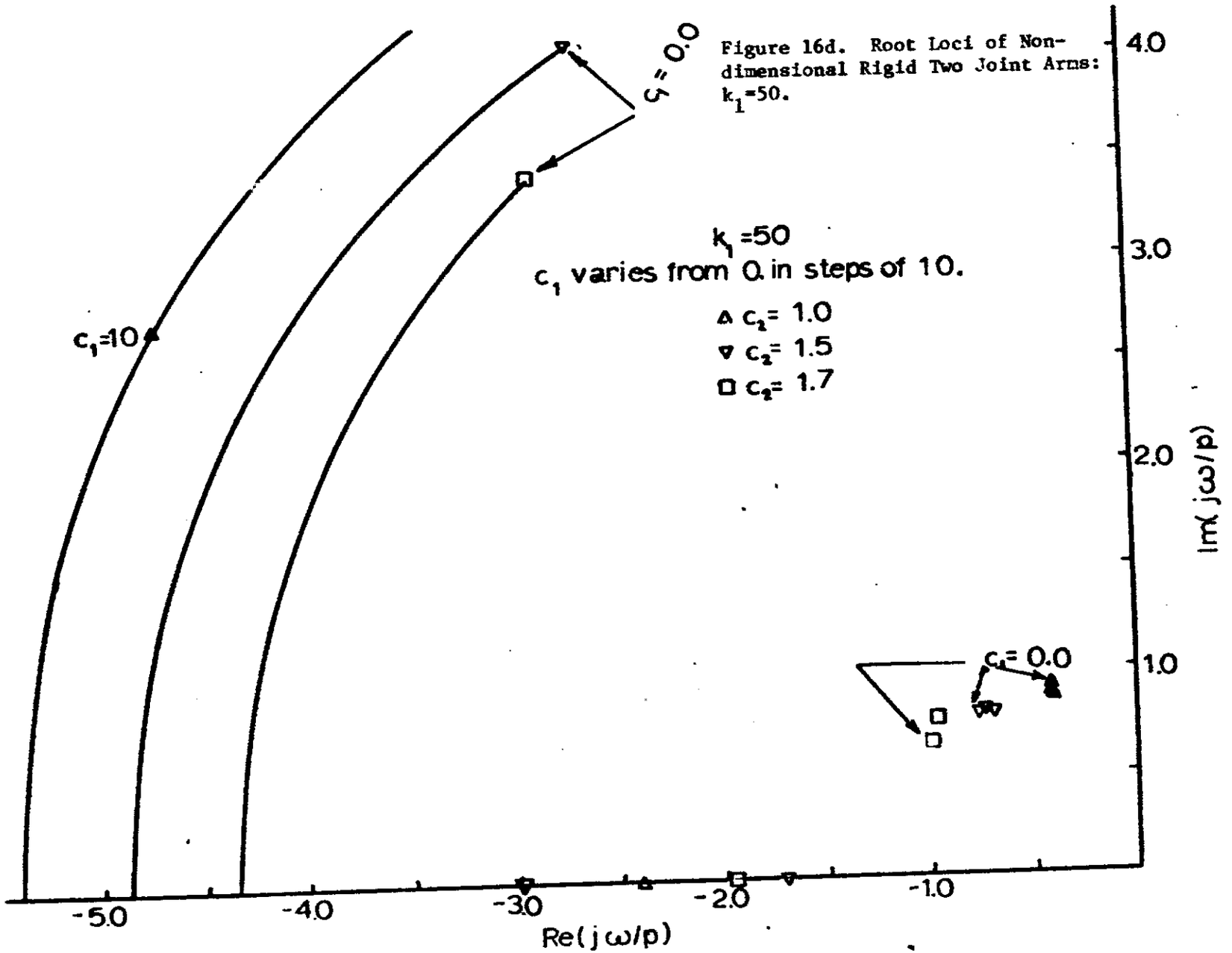

Figure 16d. Root Loci of Non-dimensional Rigid Two Joint Arms: k_1=50.

Figure 17. Variation in Roots with ω_c. Nondimensionalization by Table 7.